The Physics of Space Plasmas

Auroral and Polar Cap Phenomenology (2)

William J. Burke
19 September 2012
University of Massachusetts, Lowell

BOSTON COLLEGE
ISR
INSTITUTE FOR SCIENTIFIC RESEARCH

Lecture 4

- **This lecture deals primarily with the characteristics of high (keV) energy particles that precipitate into the high-latitude ionosphere.**
- **What do the energy spectra of high-latitude populations look like?**
  - **How do they vary with IMF's orientations?**
  - **How does one distinguish between sources of dayside populations?**
  - **What are the sources of nightside precipitating particles?**
  - **What happens when IMF B_Z turns northward?**
- **Besides the Region 1 – Region 2 system magnetometers see smaller scale FACs associated with discrete auroral formations**
  - **What do they look like in data streams and how do they come about?**
  - **What are their relationships with particle precipitation electric field patterns?**
  - **What happens in the presence of $E_{||}$?**

Aurorae and Polar Cap

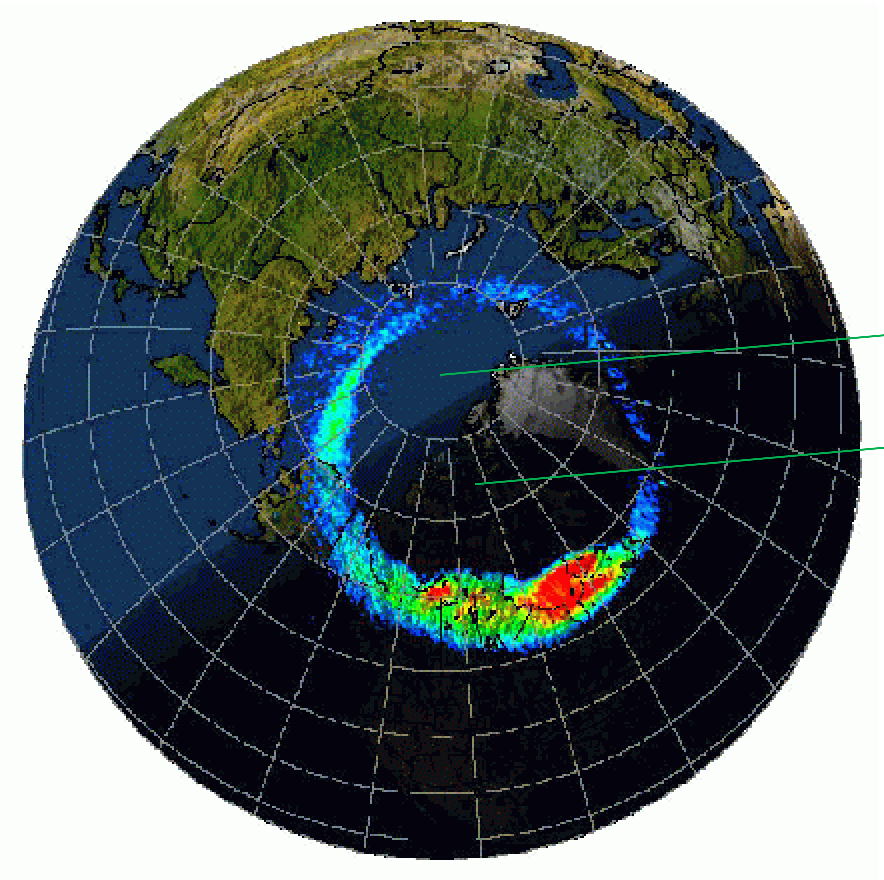

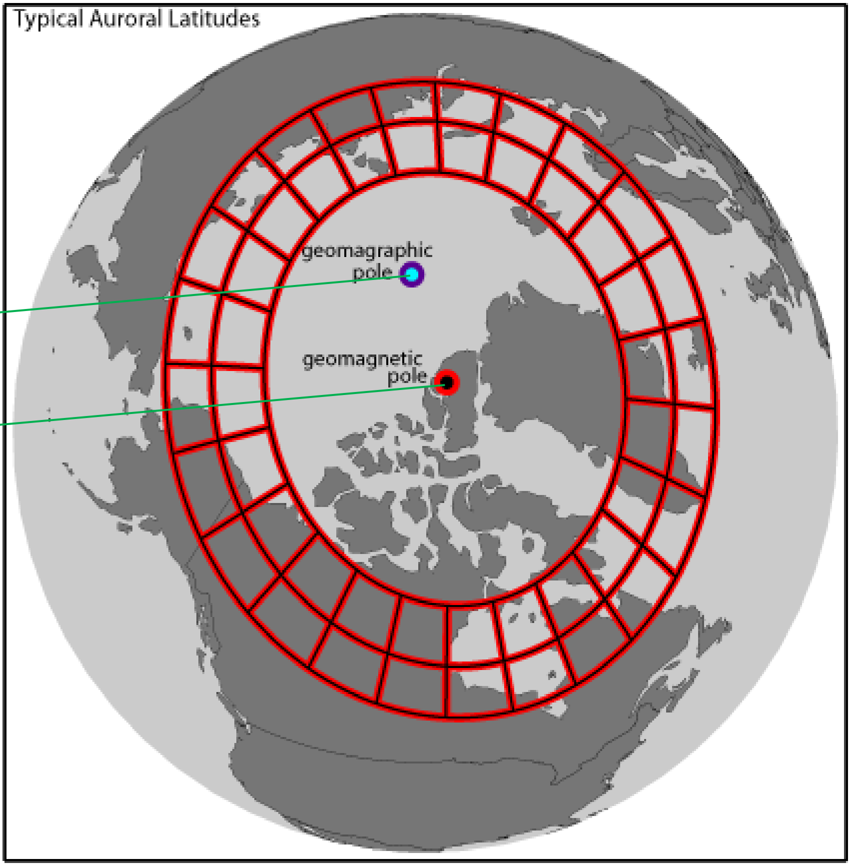

Aurorae and Polar Cap

Dayside Precipitation Pattern
***Newell and Meng*, GRL, 1992**

Dayside FAC System
***Erlandson et al.*, JGR, 1988**

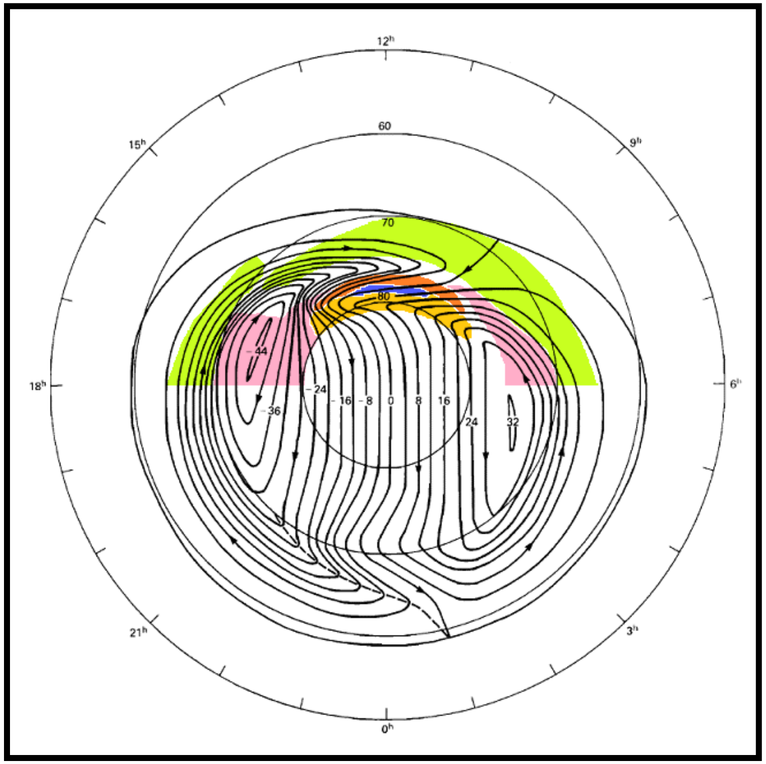

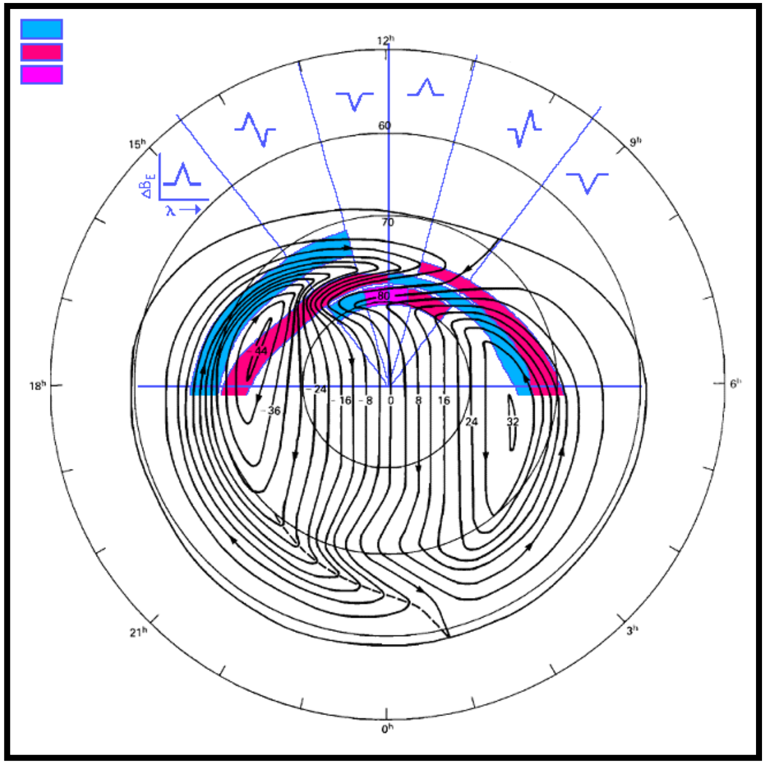

Heppner - Maynard Convection Patterns (JGR, 1987)

Aurorae and Polar Cap

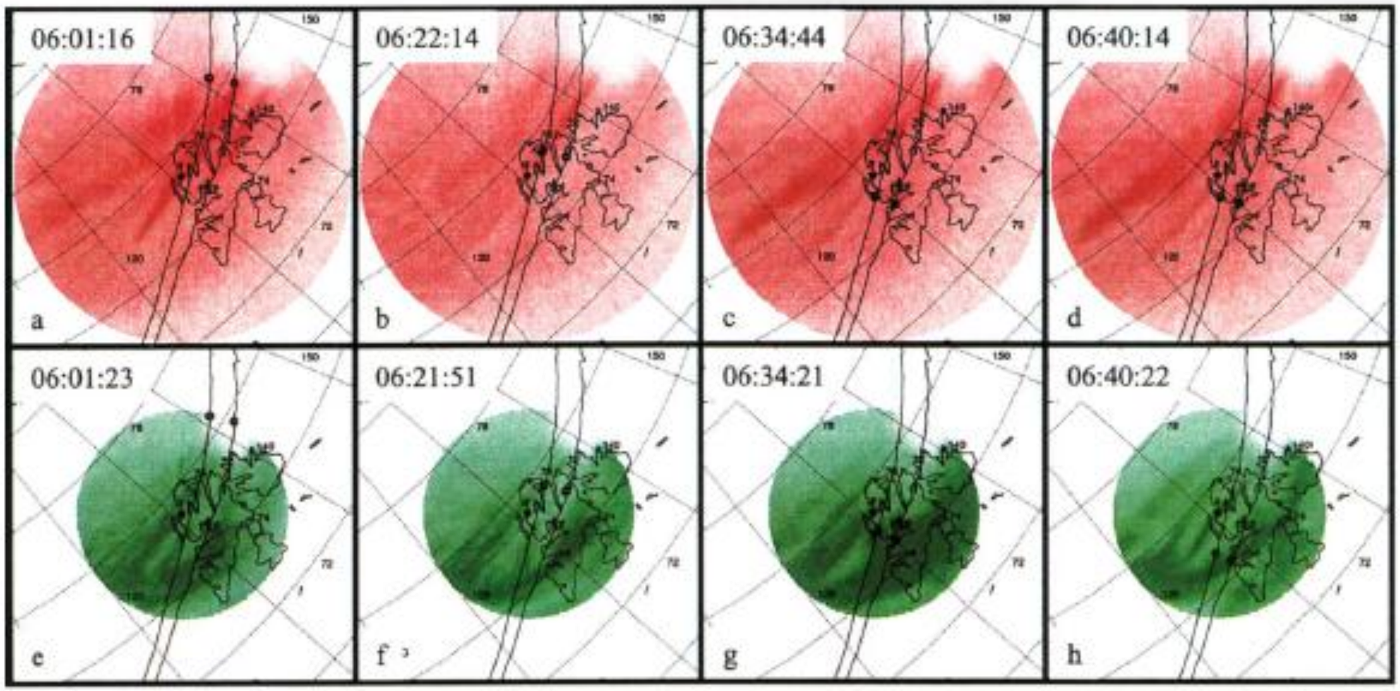

Plate 2. Time series of red 630.0-nm and green 557.7-nm ASC images for November 30, 1997. Overlapped on the plots are the foot points of Polar. A circle shows the location of Polar at the time the image was recorded. The MLT of Ny-Ålesund is MLT = UT + 3 hours.

Aurorae and Polar Cap

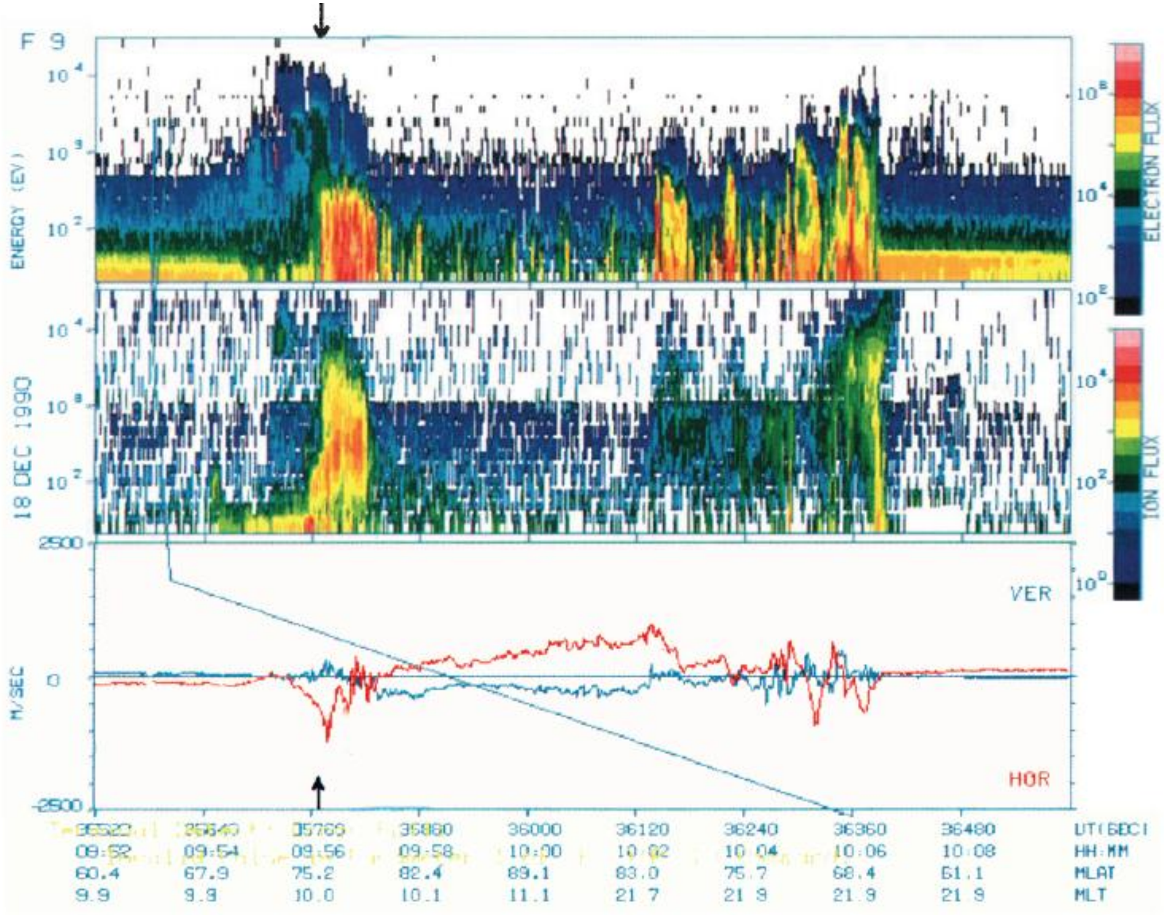

Plate 1. (top, middle) Electron and ion precipitation spectra obtained from spacecraft DMSP F9 during a polar pass along the ~10-22 MLT meridian on December 18, 1990. (bottom) Horizontal (cross-track) and vertical ion drifts marked by red and blue traces, respectively. The arrows mark the estimated location of the open/closed field line boundary at 10 MLT.

Sandholt et al. JGR 1998

Space Plasma & Field Sensors

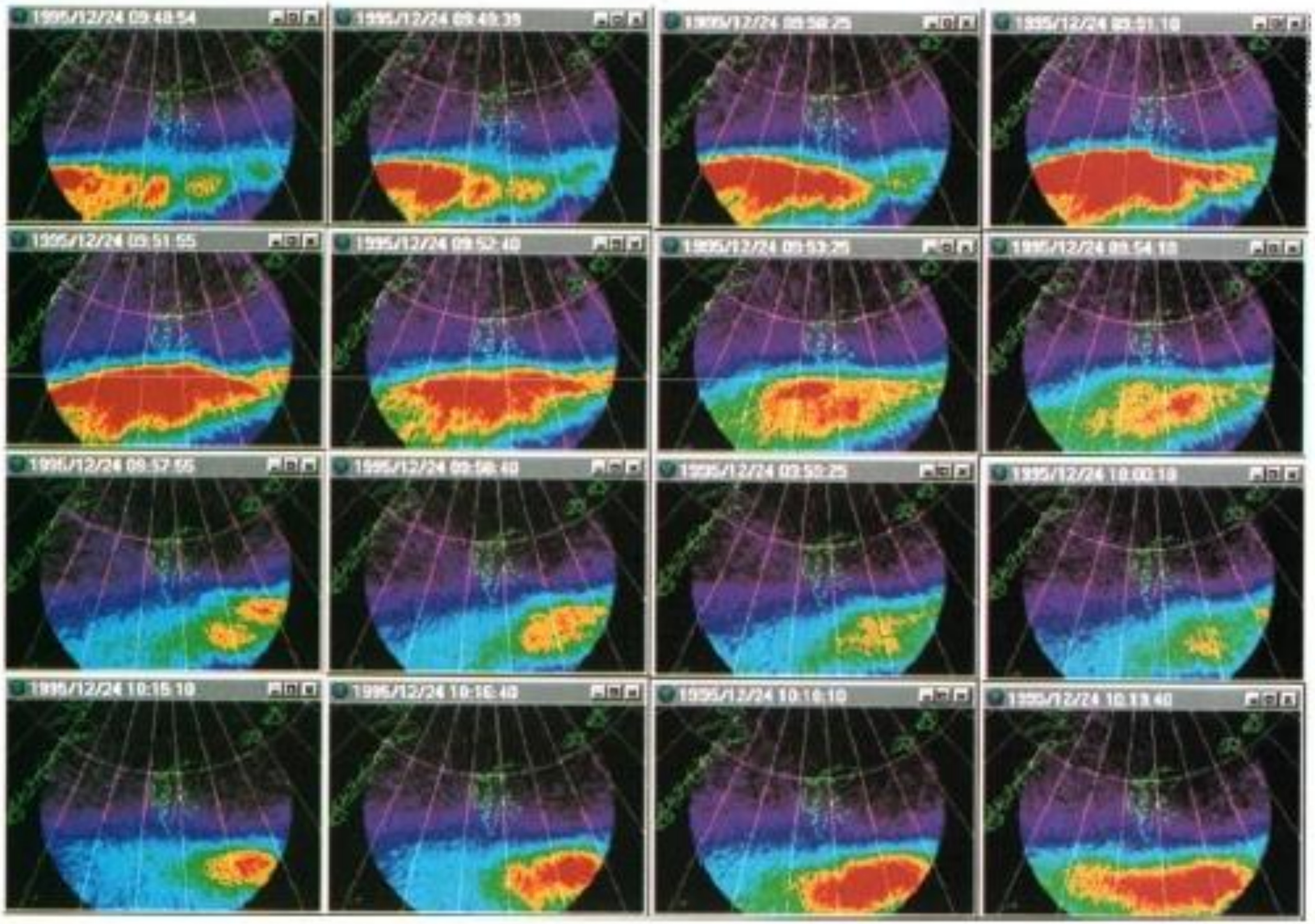

Aurorae and Polar Cap

Heppner-Maynard, JGR, 1987

Northern Hemisphere:
$B_Y > 0$, $B_Z < 0$

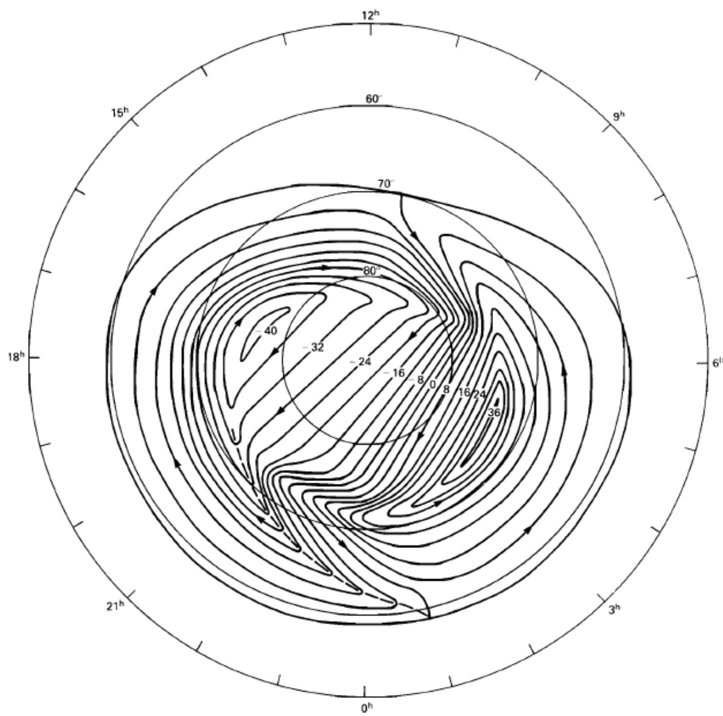

Model BC

Southern Hemisphere:
$B_Y < 0$, $B_Z < 0$

Northern Hemisphere :
$B_Y < 0$, $B_Z < 0$

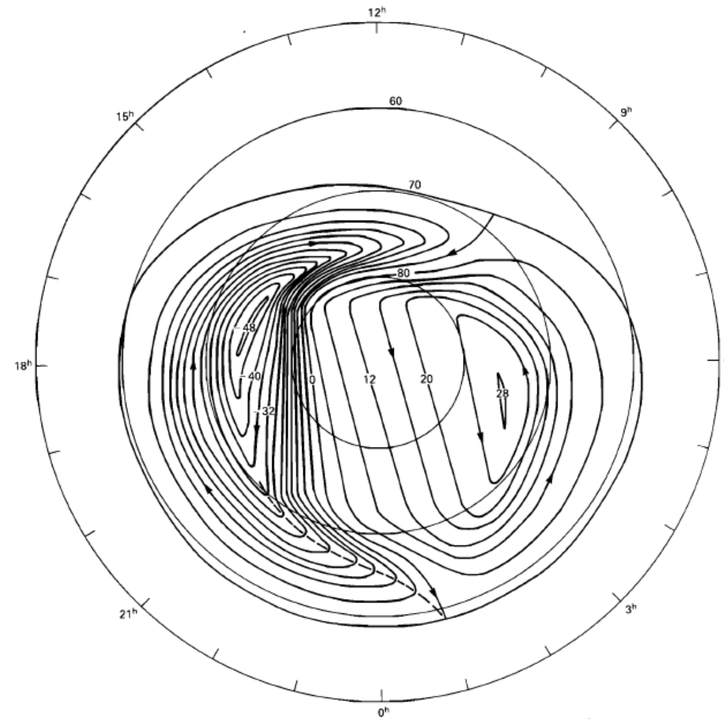

Model DE

Southern Hemisphere:
$B_Y > 0$, $B_Z < 0$

Aurorae and Polar Cap

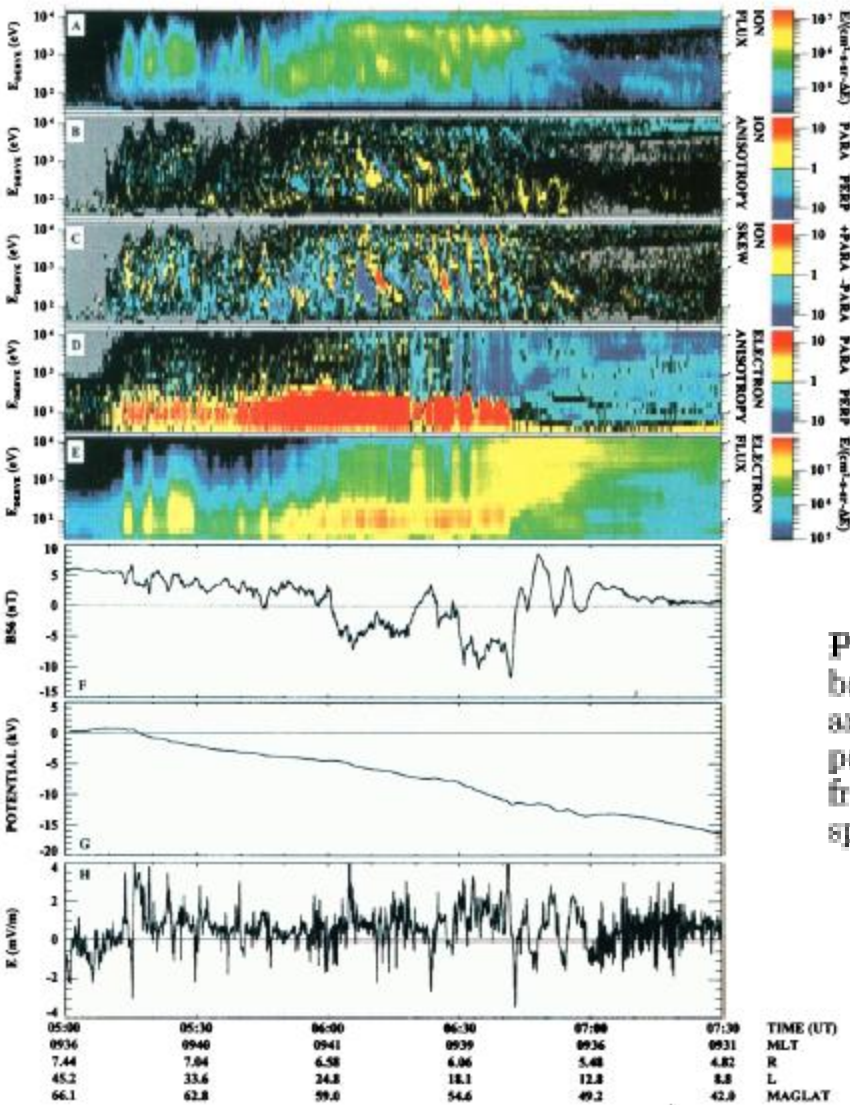

Plate 1. Polar/Hydra data for November 30, 1997, from 0500 t
bottom the energy time spectrograms for (a) ions, (b) ion aniso
anisotropy, (e) electrons, (f) B56 component of the magnetic fiel
potential and (h) electric field component along the spacecraft
frame of reference. The B56 component of the magnetic fiel
spacecraft and is positive westward.

Aurorae and Polar Cap

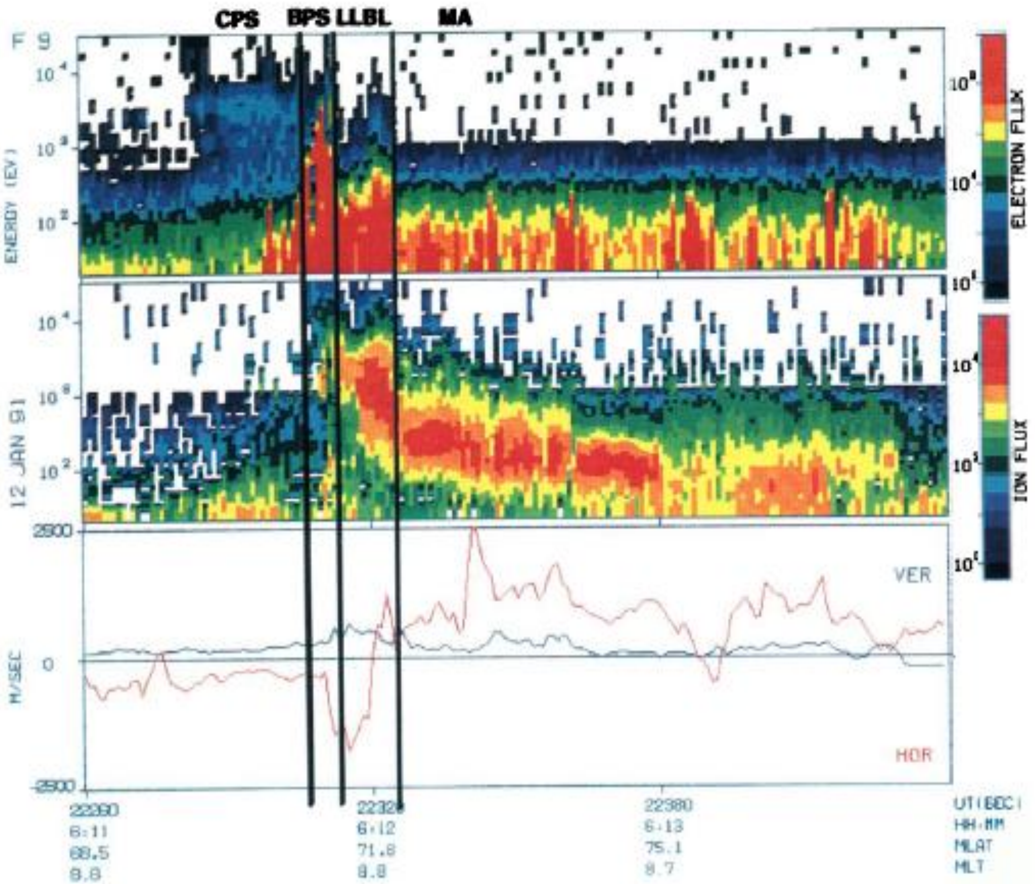

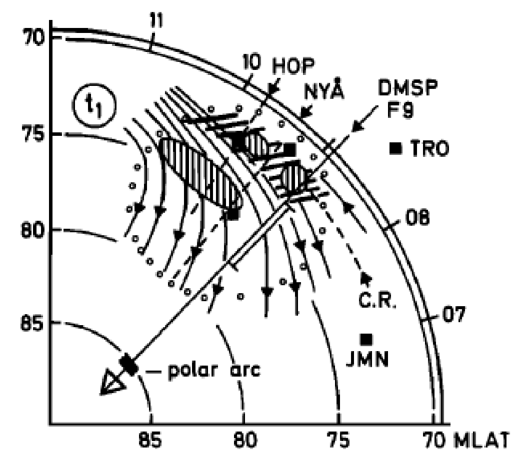

Plate 4. The top two panels show DMSP F9 electron and ion precipitation spectra along the ~09 MLT meridian. Horizontal (east-west) and vertical (blue) ion drifts are plotted in the bottom panel. Note the convection reversal at 71.8° MLAT and the westward flow within the region of energy versus latitude dispersion of ion precipitation (73°–79° MLAT).

***Sandholt et al.*, JGR 1993**

Aurorae and Polar Cap

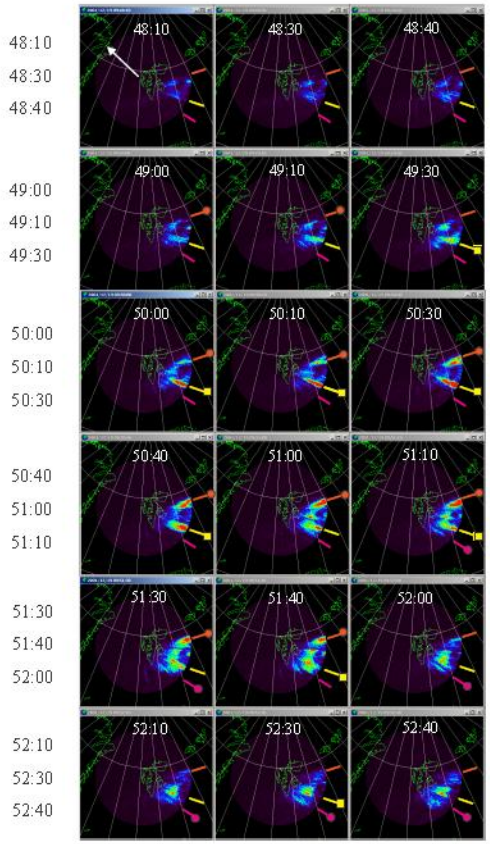

Ny-Ålesund: 09+ UT, December 19, 2001

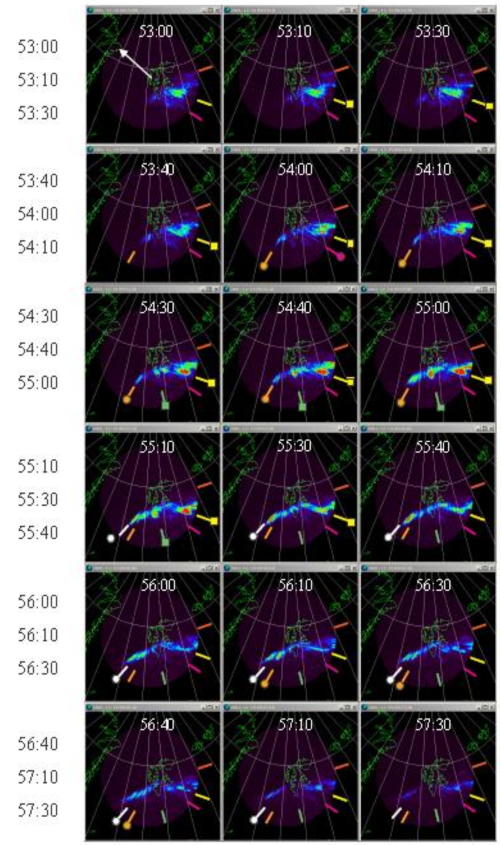

Ny-Ålesund: 09+ UT, December 19, 2001

5577 Å emissions monitored by all-sky imager at Ny Ålesund after 09:00 UT on 19 December 2001. The colored lines are placed at constant positions as guide to the eye for discerning optical changes.

Aurorae and Polar Cap

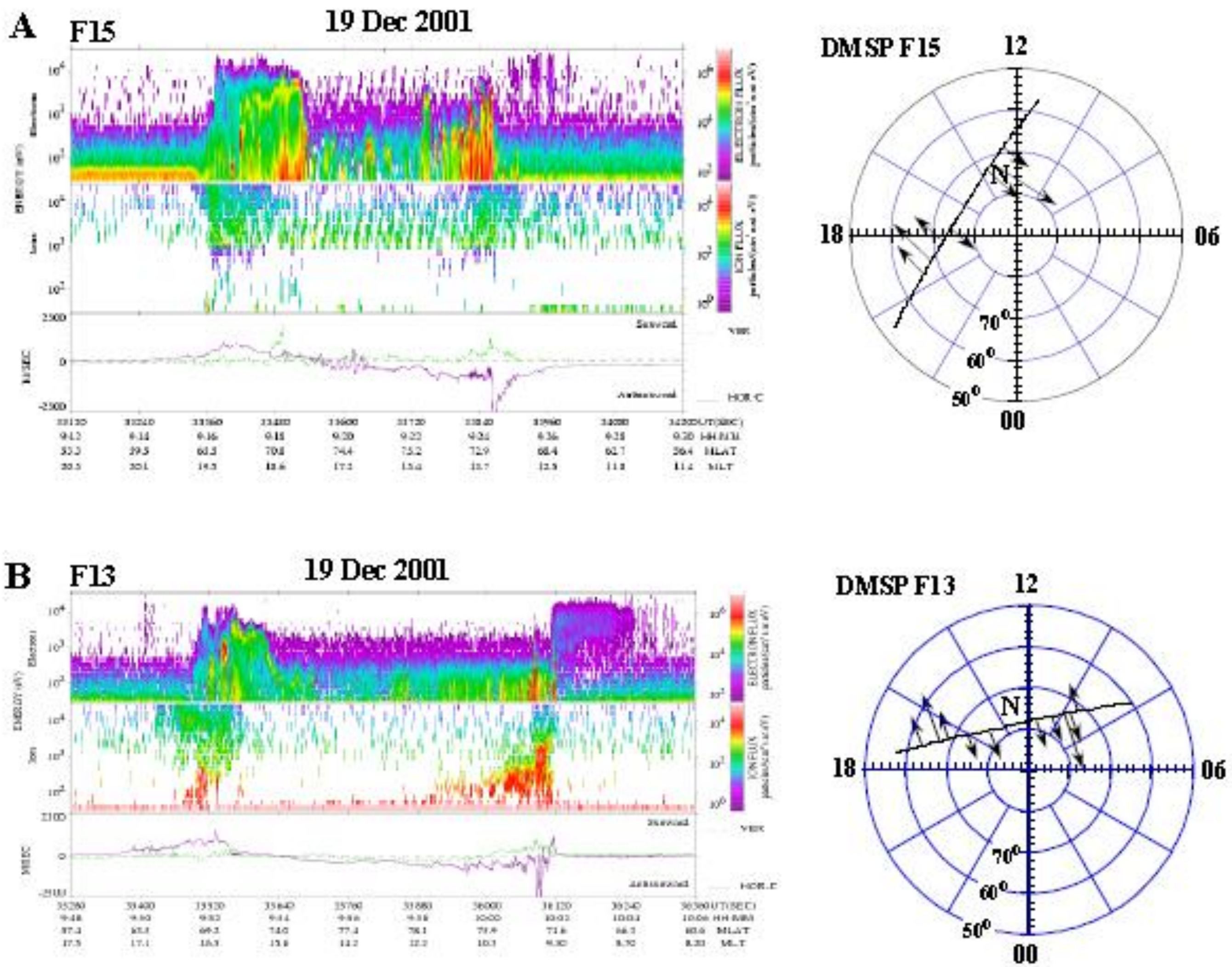

F15 / F13 crossed local noon MLT at ~ 09:22 an 09:36 UT

Aurorae and Polar Cap

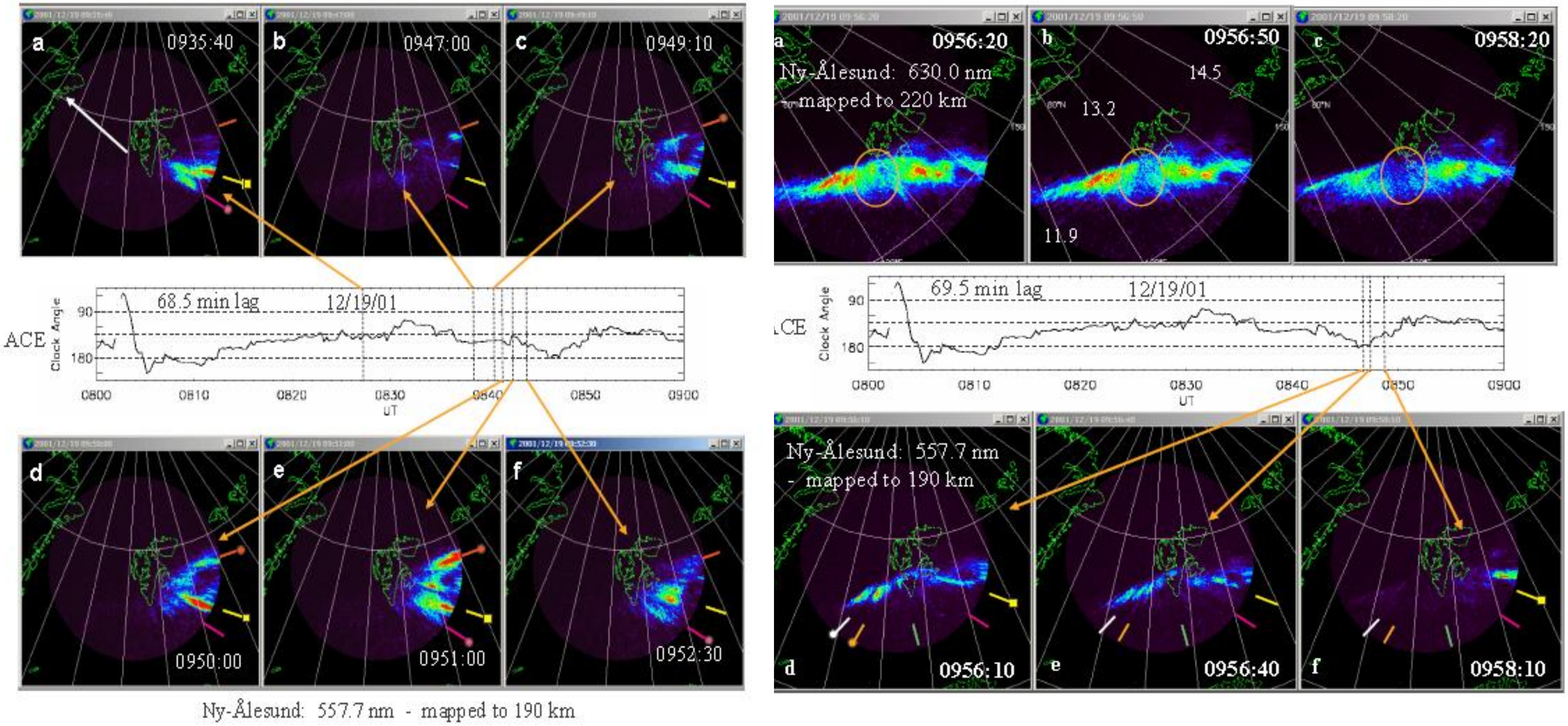

Top right: 6300 Å emissions mapped to 220 km. All 5577 Å emissions mapped to an altitude of 190 km. Middle traces indicate that 5577 Å variations are responses to changes in the IMF clock angle.

Aurorae and Polar Cap

Comparison of two SuperDARN coherent back scatter patterns with images from all-sky monitor at Ny Ålesund on 19 December 2001.

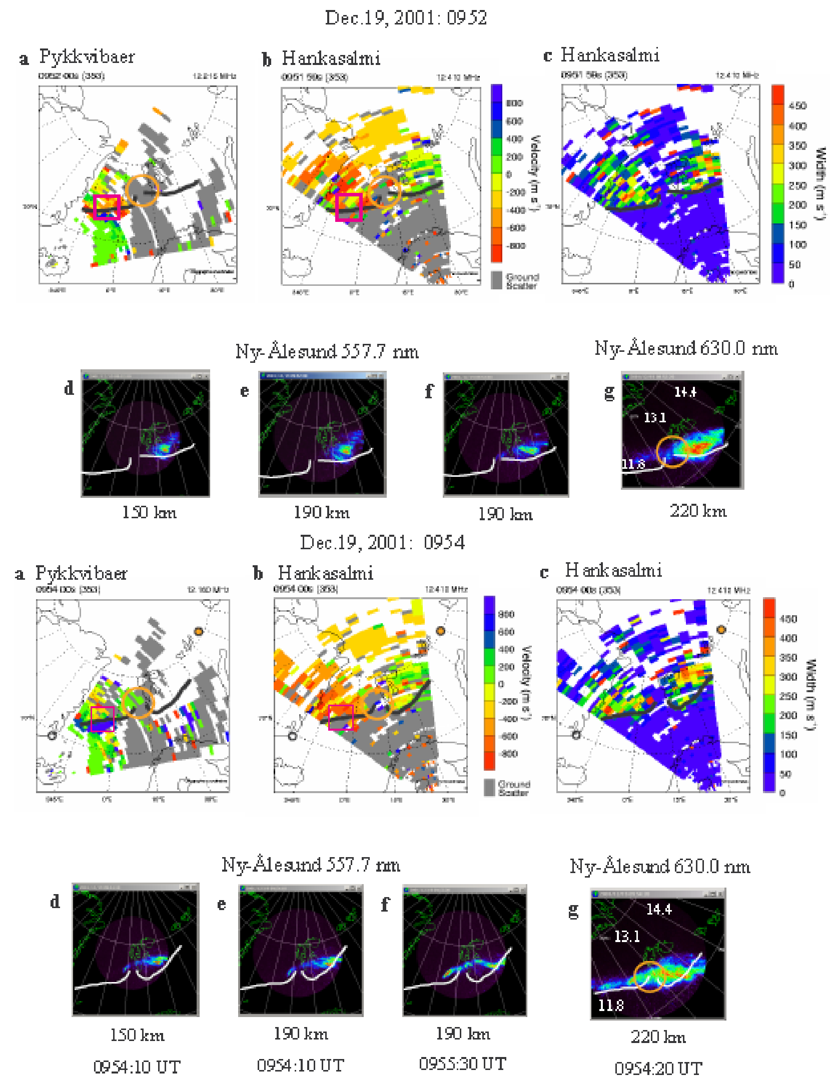

Aurorae and Polar Cap

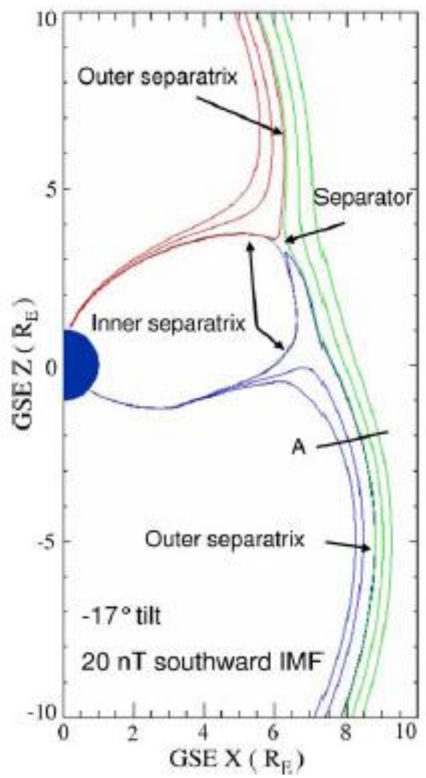

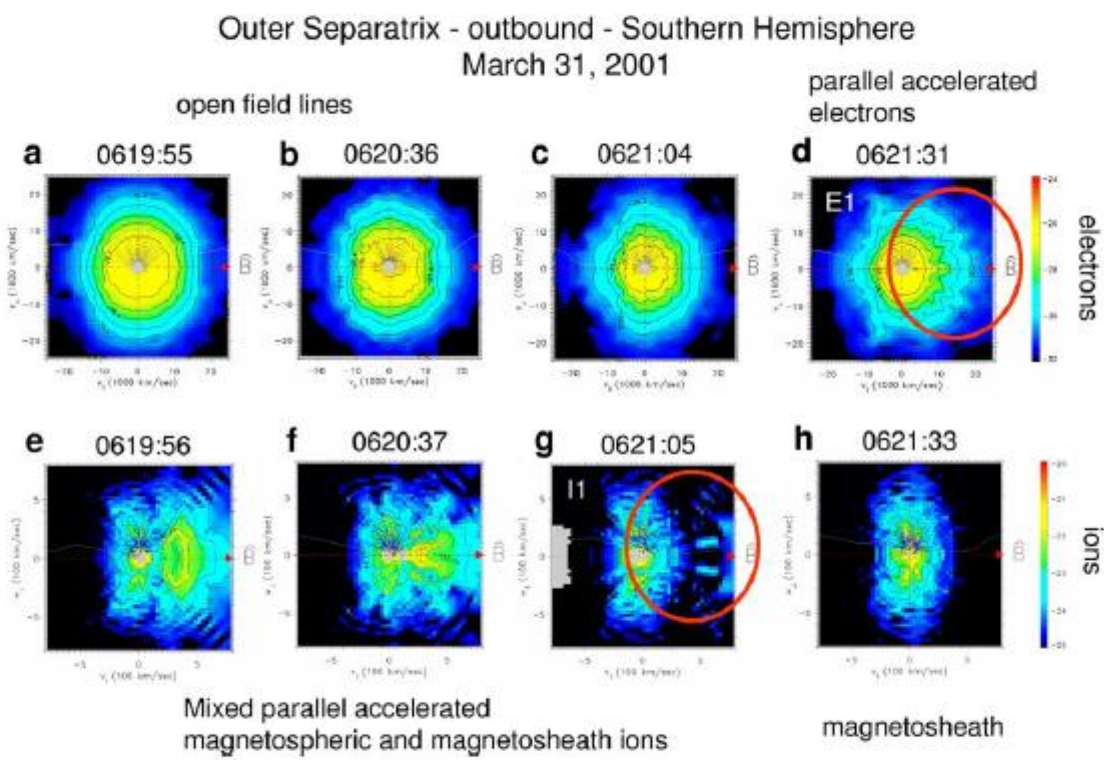

On 31 March 2001 Polar was in a skimming orbit along the dayside magnetopause Where it encountered debris from active merging sites => detected field aligned beams of keV electrons moving along the separatrices. These electrons excite 5577 Å emission at equatorward boundary of the cusp.

Aurorae and Polar Cap

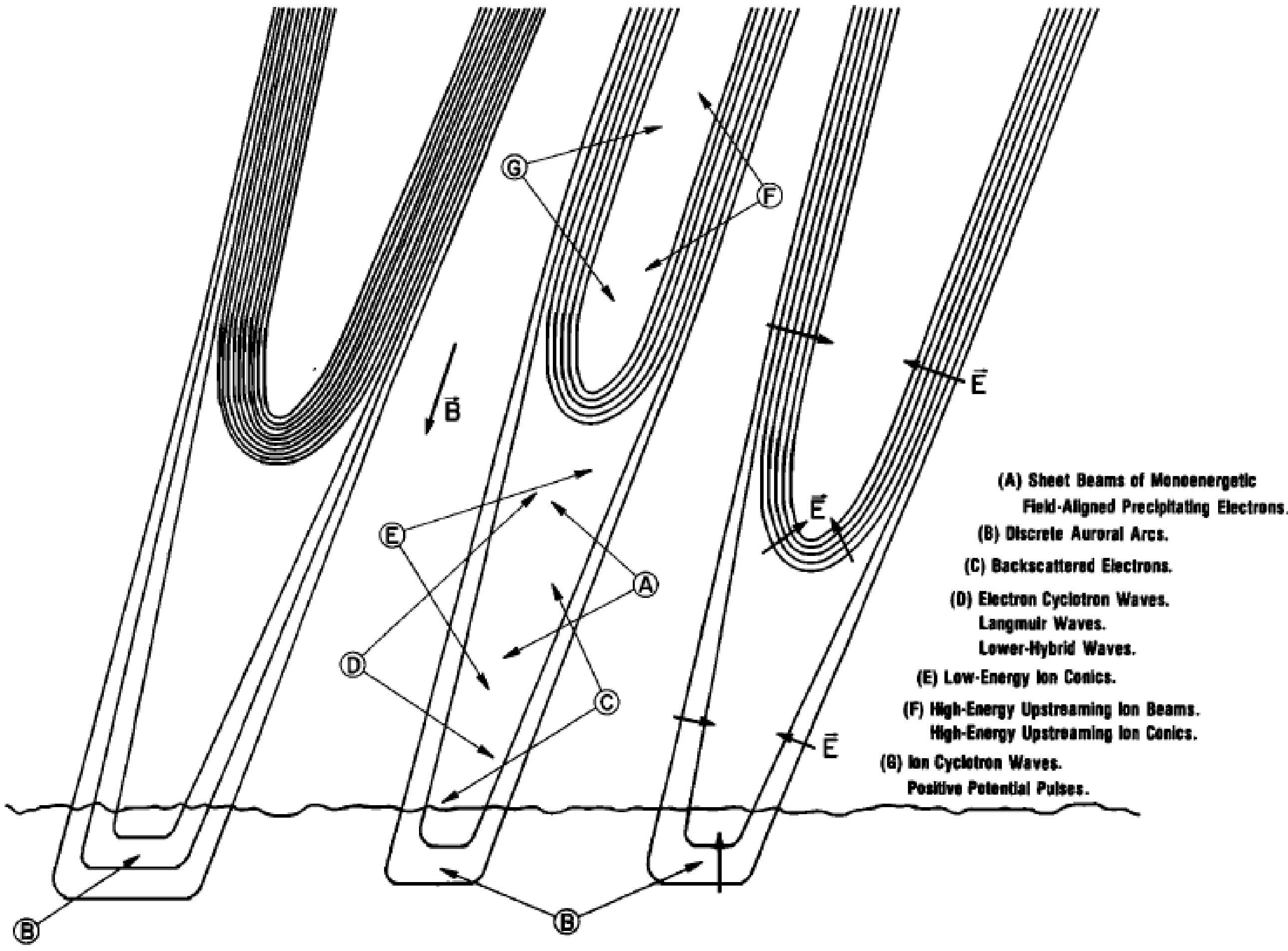

Fig. 1. A schematic (not to scale) of the equipotential contours and related phenomena above a multiple auroral arc as seen in a north-south cut.

Borovsky JGR 1984

Aurorae and Polar Cap

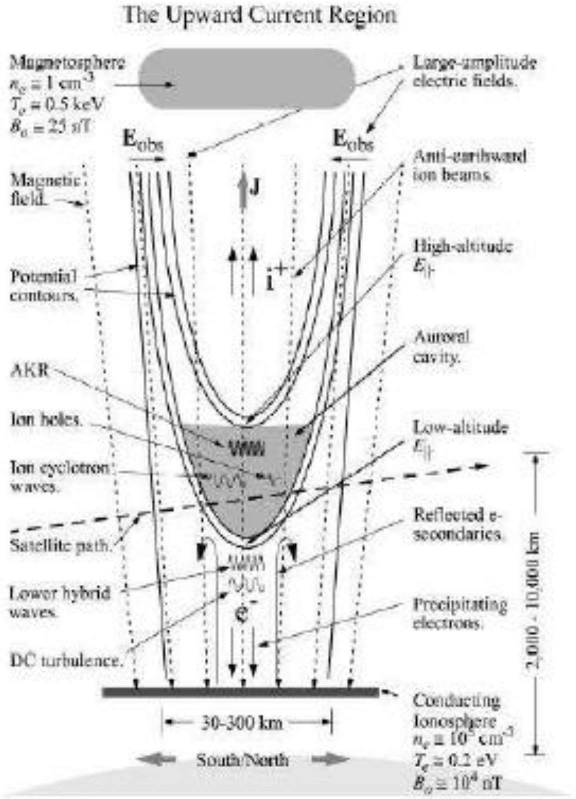

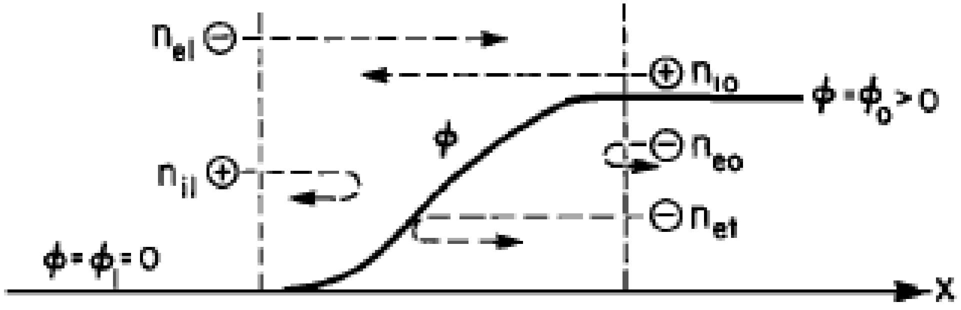

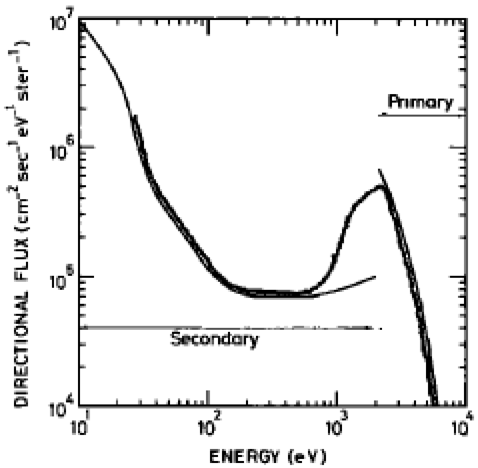

Fridman, M., and J. Lemaire, JGR, 664, 1980.
Kan and Lee, JGR, 788, 1979.

Aurorae and Polar Cap

• Consider a trapped electron population with an isotropic, Maxwellian distribution function whose mean thermal energy = E_{th}

• Assume that there is a field-aligned potential drop $V_{||}$ that begins at a height where the magnetic field strength is $B_{V||}$.

• ***Knight*** **(PSS, 741, 1973) showed that** $j_{||}$ **carried by precipitating electrons is given by the top equation, where** B_i **is the magnetic field strength at the ionosphere.**

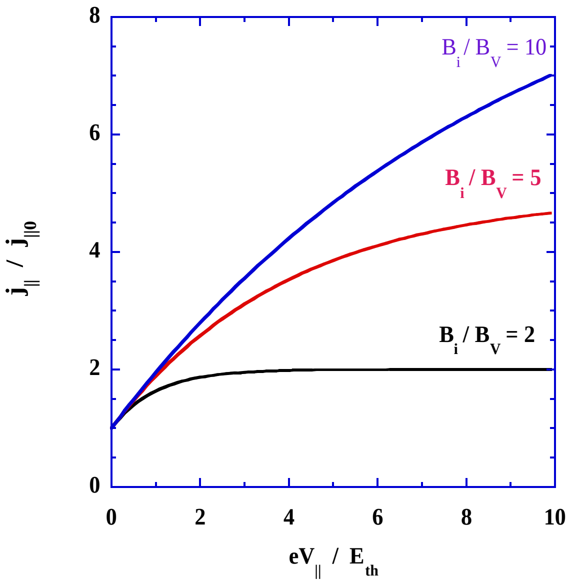

***Lyons*, JGR, 17, 1980**

$j_{||}$ - $V_{||}$ Relationship

$$j_{||} = en\left(\frac{E_{th}}{2\pi m_e}\right)\frac{B_i}{B_{V_{||}}}\left[1-\left(1-\frac{B_{V_{||}}}{B_i}\right)\exp\left\{\frac{-eV_{||}/E_{th}}{(B_i/B_{V_{||}}-1)}\right\}\right]$$

Let

$$j_{||0} = en\left(\frac{E_{th}}{2\pi m_e}\right)$$

then

$$j_{||} = j_{||0}\frac{B_i}{B_{V_{||}}}\left[1-\left(1-\frac{B_{V_{||}}}{B_i}\right)\exp\left\{\frac{-eV_{||}/E_{th}}{(B_i/B_{V_{||}}-1)}\right\}\right]$$

If

$$V_{||} = 0$$

or

$$B_{V_{||}} = B_i$$

$$j_{||} = j_{||0}$$

Aurorae and Polar Cap

Equivalent current system and external driving with IMF $B_Z > 0$
***Maezawa*, JGR, 2289. 976**

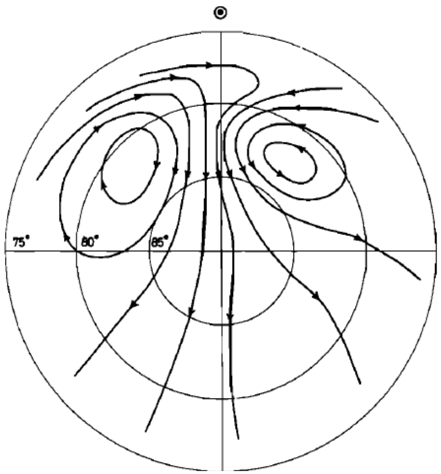

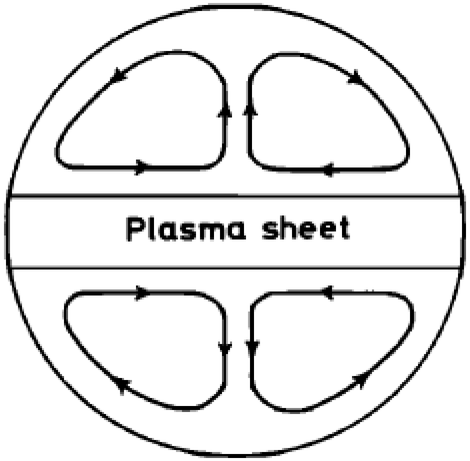

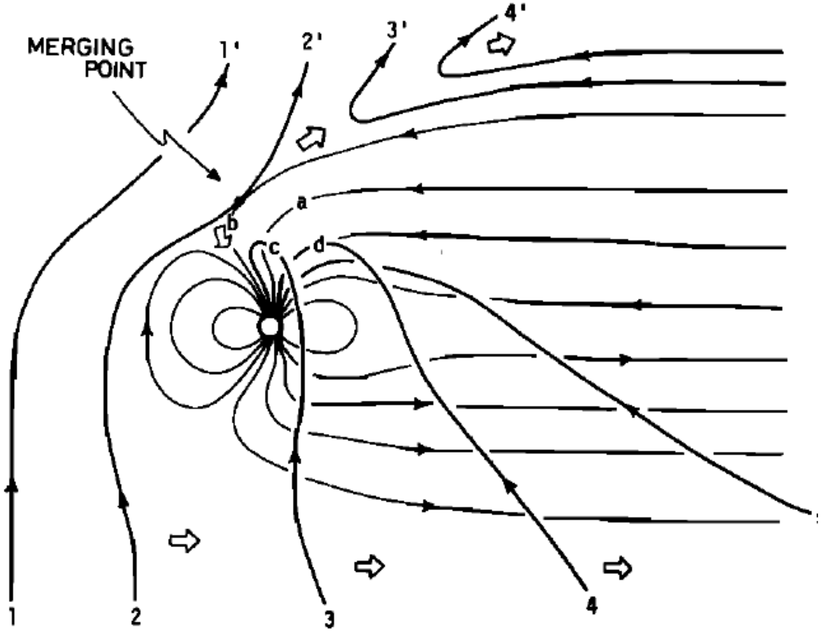

Aurorae and Polar Cap

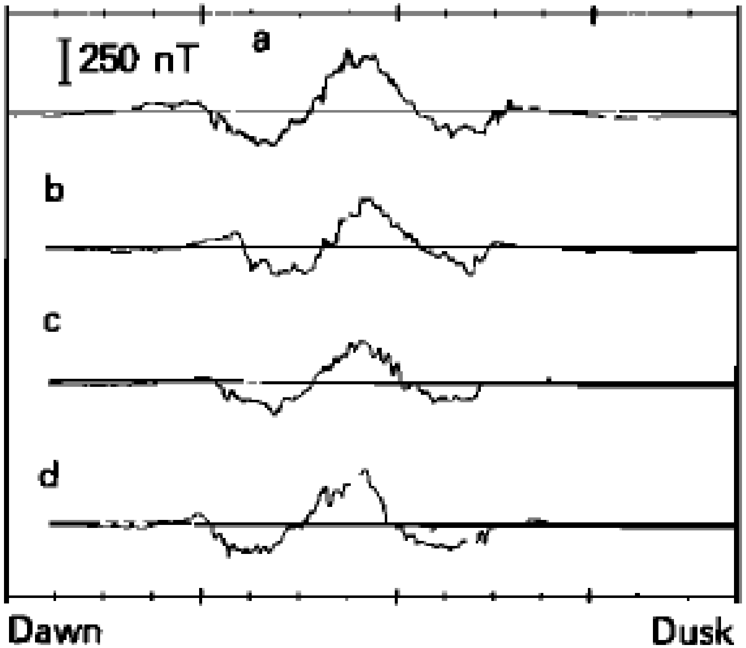

MAGSAT ΔS measurements from four southern high-latitude passes on 8 Jan. 1980

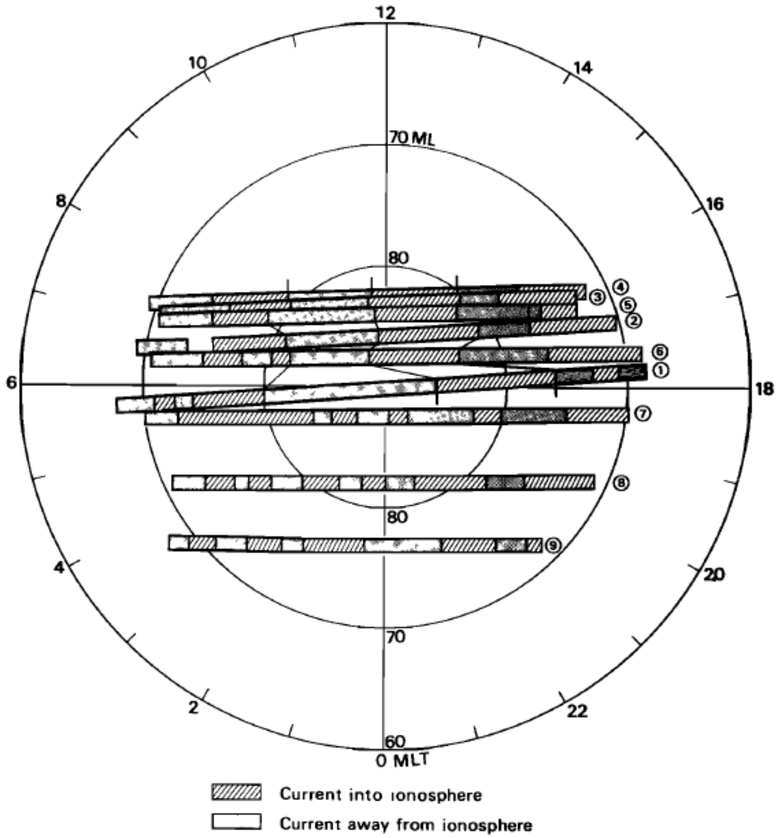

NBZ current system

Aurorae and Polar Cap

Ion Velocity Dispersion Effect

Dungey, 1961

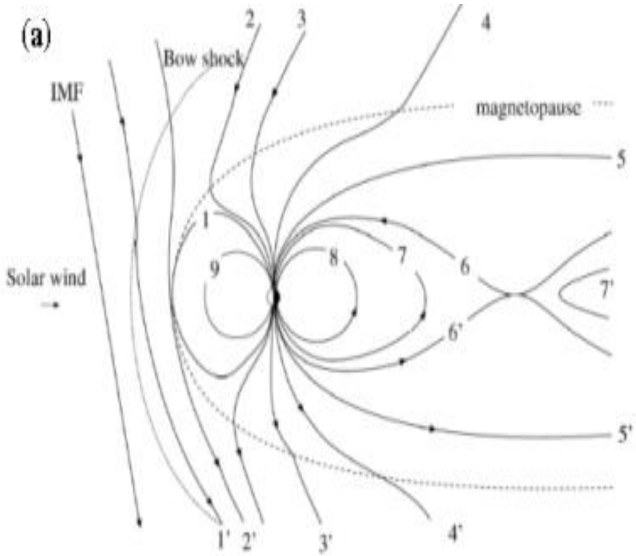

IMF $B_Z < 0$

Highest energy ions at equatorward boundary of the cusp

Maezawa, 1976

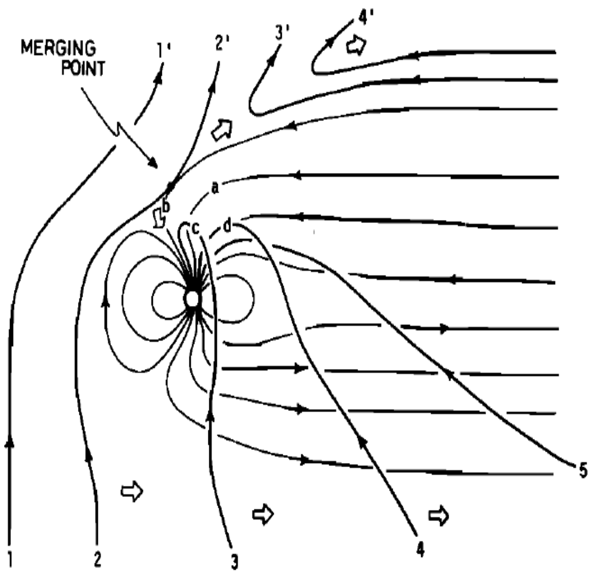

IMF $B_Z > 0$

Highest energy ions at poleward boundary of the cusp

Aurorae and Polar Cap

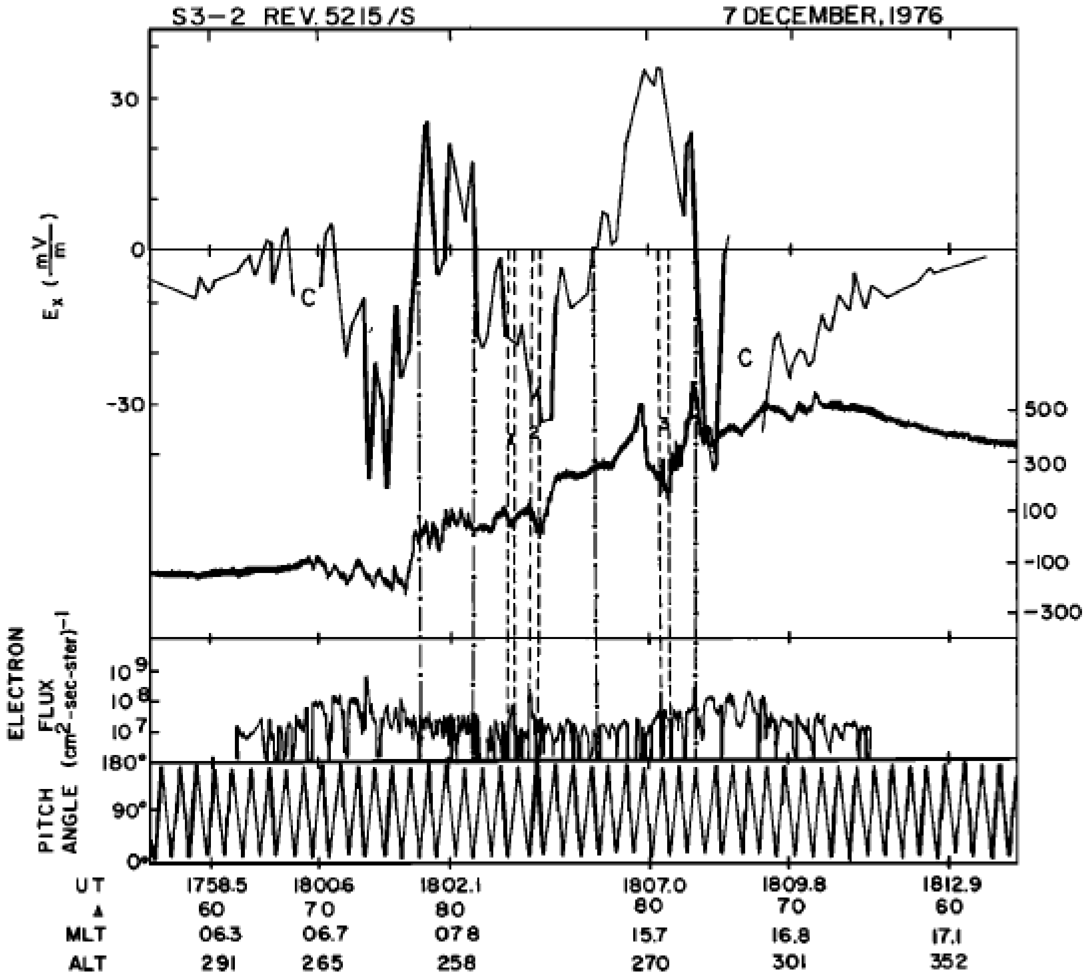

. Electric field, magnetic field, electron flux, and pitch angle measurements during S3-2 rev 5215S. The format is the same as for Figure 1. Hourly averaged IMF components were 3.6, −2.8, and 4.1 nT.

Aurorae and Polar Cap

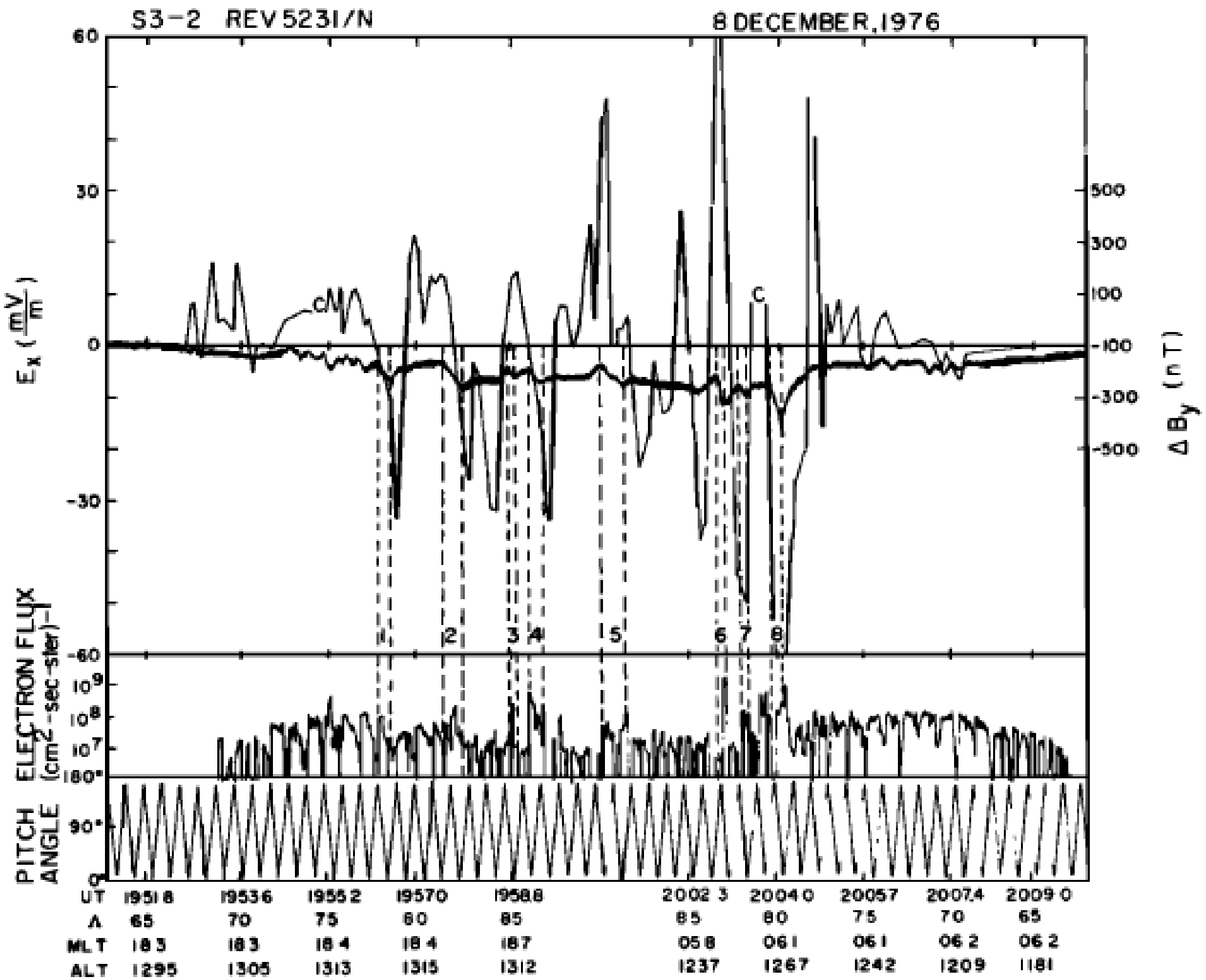

Fig. 1. Electric field, magnetic field components, the directional electron flux, and pitch angle as functions of UT, invariant latitude, magnetic local time, and altitude from S3-2 rev 5231N. Eight events marked by field-aligned currents out of the ionosphere are denoted by dashed lines. At the time of this pass the hourly averaged values of the IMF X, Y, and Z solar magnetospheric components were −3.7, 4.4, and 7.1 nT, respectively.

Aurorae and Polar Cap

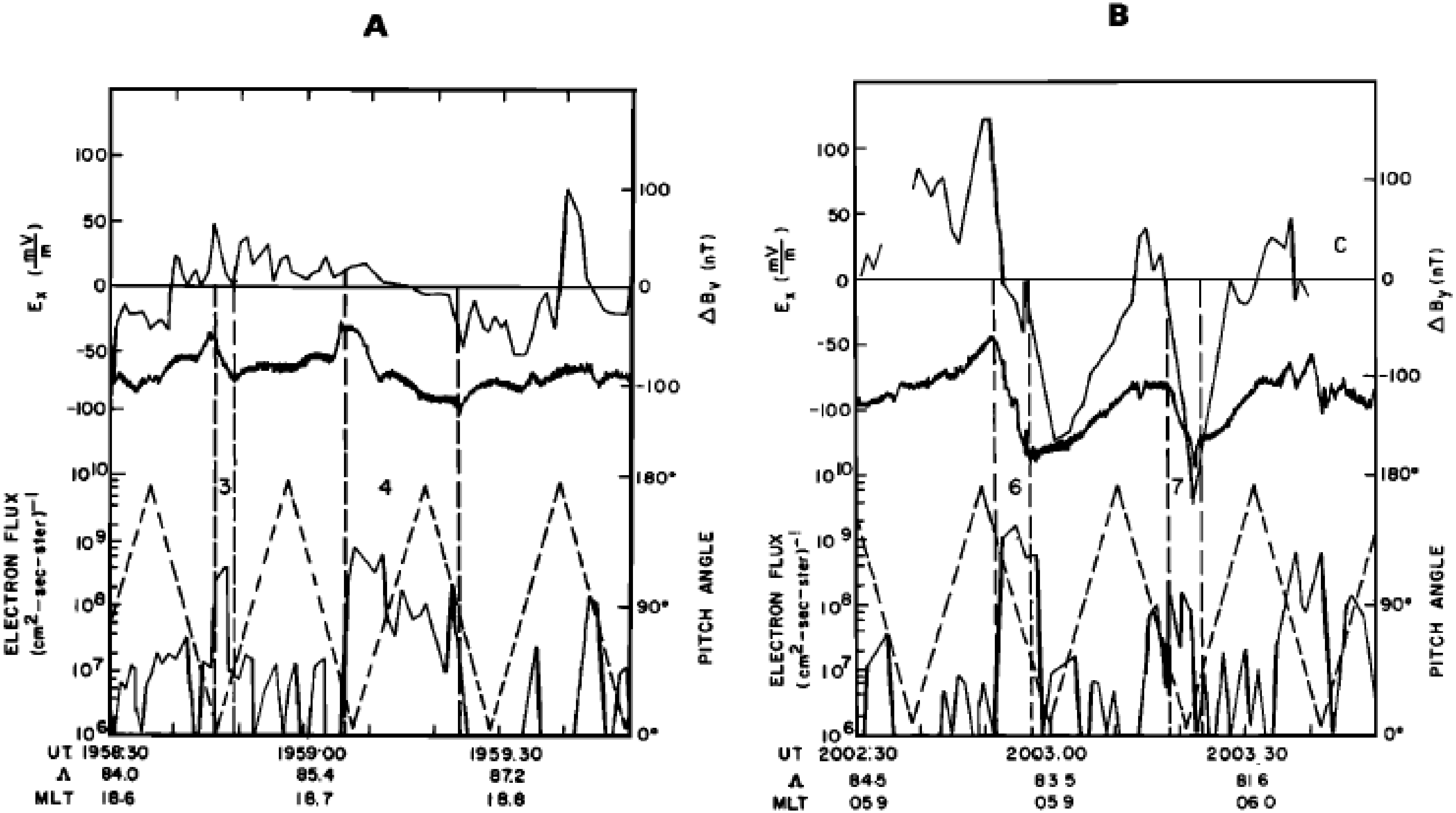

Fig. 3. One-second average of E_x deduced from potential measurements in Figure 2: (*a*) from period of events 3 and 4 and (*b*) from period of events 6 and 7.

Aurorae and Polar Cap

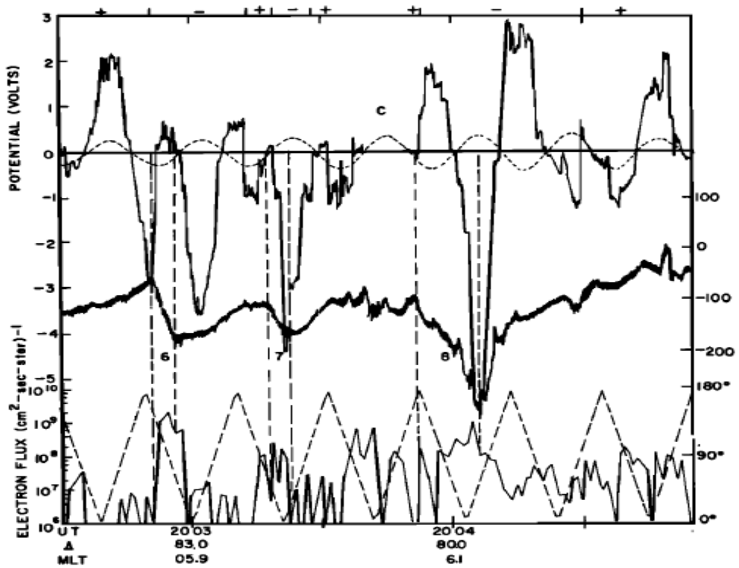

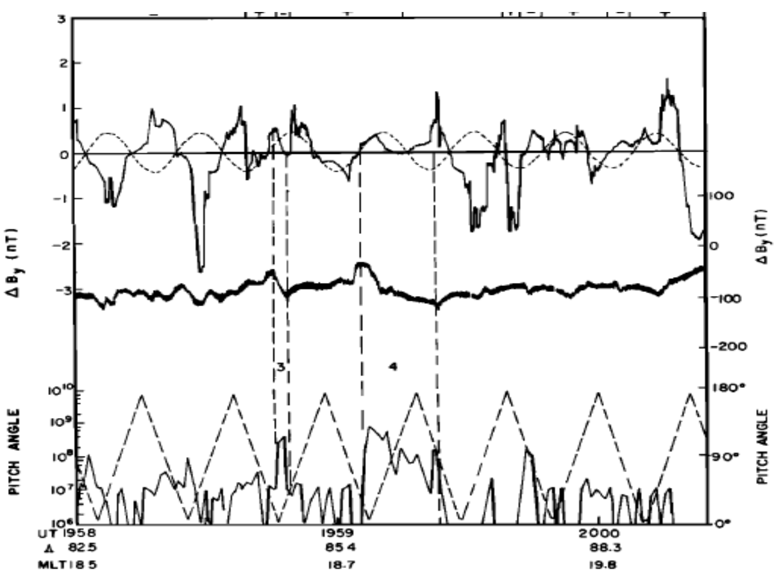

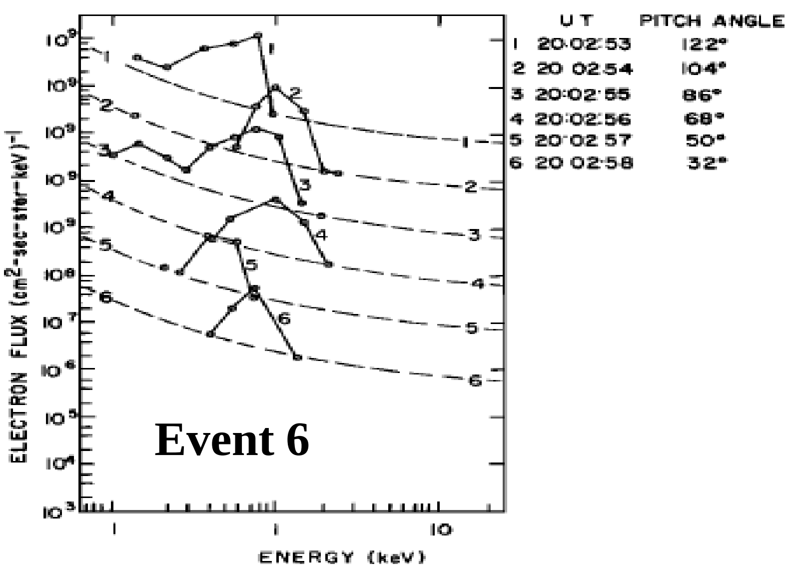

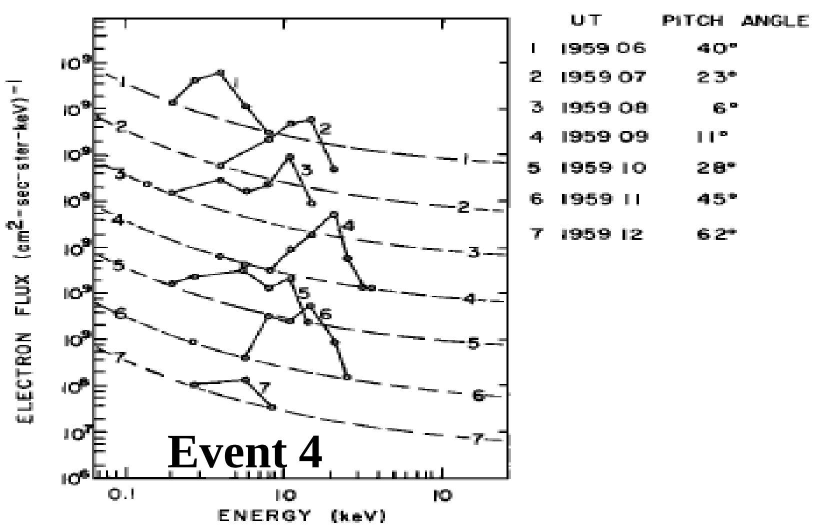

Aurorae and Polar Cap

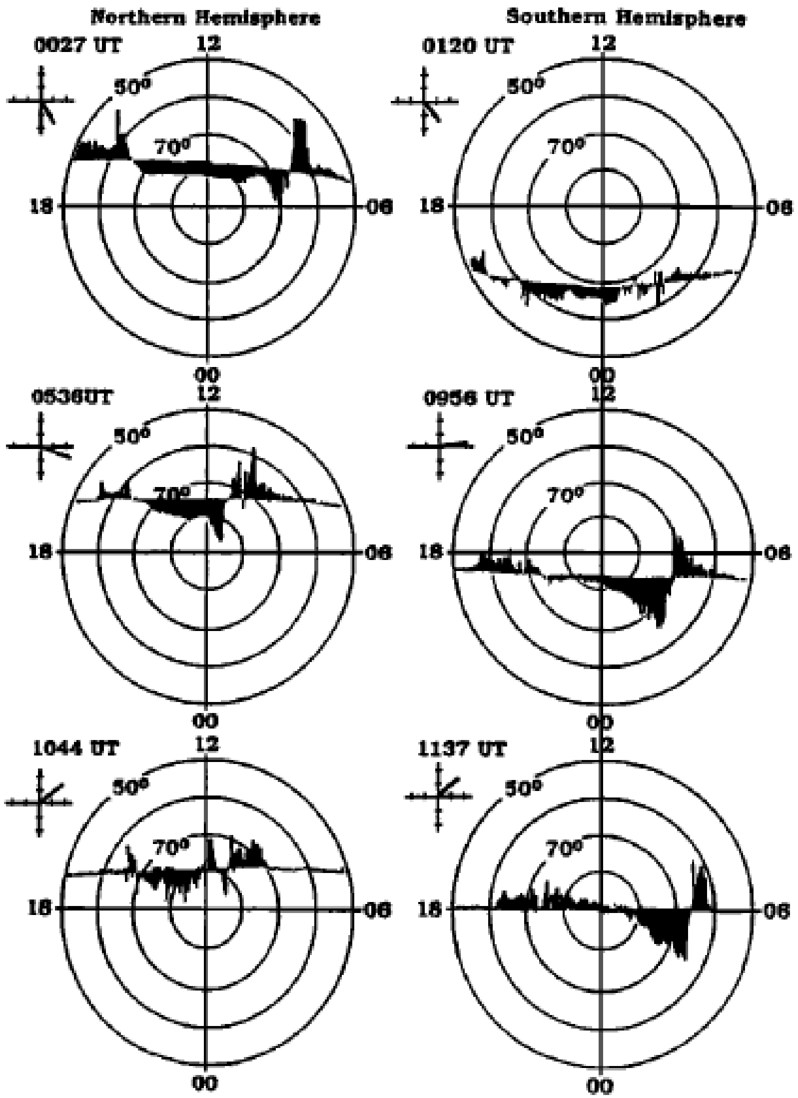

Figure 1. DMSP ion drift measurements from three northern and southern high-latitude passes during southward–westward IMF interval. Data are plotted in Λ versus MLT coordinates. The UT to the left of each plot refers to satellite crossings of the magnetic noon-midnight meridian. Also indicated are hourly IMF averages, in the hour prior to the DMSP measurements, projected onto the Y_{GSM}–Z_{GSM} plane.

Table 1. Southward and Westward IMF Intervals

Date/UT	Λ_{max}	Φ_A	Φ_M	$\Delta\Phi$	$\Delta\Phi_W$	$\delta\Phi$
18/1831	82° (s/D)	-17	18	35	55	26
18/1923	86° (n/D)	-41	37	78	96	60
18/2012	86° (s/N)	-80	19	99	145	125
18/2105	83° (n/D)	-101	60	161	212	203
18/2154	80° (s/N)				209	157
18/2247	80° (n/D)	-82	84	166	207	182
18/2336	78° (s/N)	-38	41	79	204	111
19/0027	77° (n/D)	-83	91	174	194	157
19/0120	68° (s/N)	-35	34	69	156	77
19/0210	75° (n/D)	-48	96	144	170	118
19/0303	65° (s/N)	-31	23	54	166	65
19/0353	75° (n/D)	-46	59	105	170	100
19/0448	67° (s/N)	-28	18	46	138	65
19/0536	75° (n/D)	-32	76	108	129	68
19/0630	72° (s/N)	-1	62	63	125	80
19/0718	76° (n/D)	-37	60	97	115	71
19/0815	75° (s/N)	-58	88	146	115	78
19/0902	77° (n/D)	-41	34	75	92	56
19/0956	83° (s/N)	-67	64	131	117	97
19/1044	80° (n/D)	-12	57	69	83	50
19/1137	89° (s/N)	-86	31	117	75	

Aurorae and Polar Cap

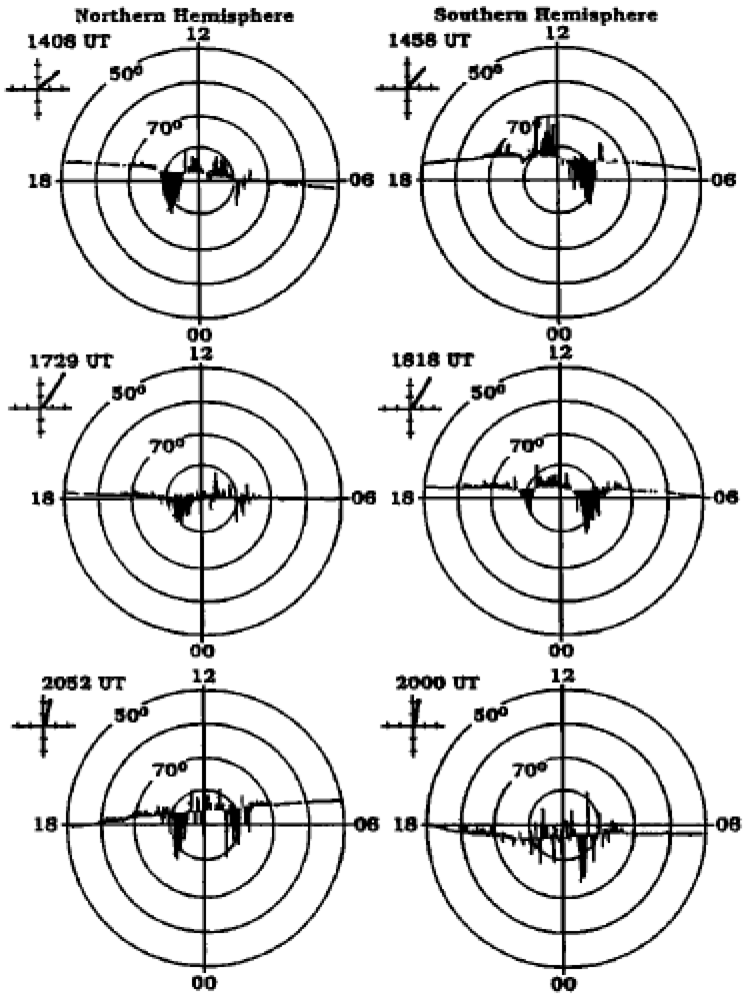

Figure 2. DMSP ion drift measurements from three northern and southern high-latitude passes of the northward IMF interval in the Figure 1 format.

Table 2. Northward IMF Intervals

Date/UT	Λ_{max}	Φ_A	Φ_M	Φ_{AL}	Φ_{ML}
19/1226	84° (n/D)	-24	4	20	
19/1318	85° (s/D)				-64
19/1408	87° (n/D)	-20		38	-9
19/1458	83° (s/D)	-5	3		-50
19/1548	89° (n/D)	-22		19	-5
19/1638	85° (s/D)	-11	8	4	-37
19/1729	89° (n/N)	-15	4	13	-7
19/1818	87° (s/D)	-7	11		-42
19/1911	88° (n/D)	-16		20	
19/2000	86° (s/N)	-12	11	11	-12
19/2052	85° (n/D)	-21	8	13	-15
19/2140	80° (s/N)	-13	9		
19/2234	82° (n/D)	-11		14	-20
19/2324	74° (s/N)	-5	12		

Aurorae and Polar Cap

Dayside Precipitation Pattern
***Newell and Meng*, GRL, 1992**

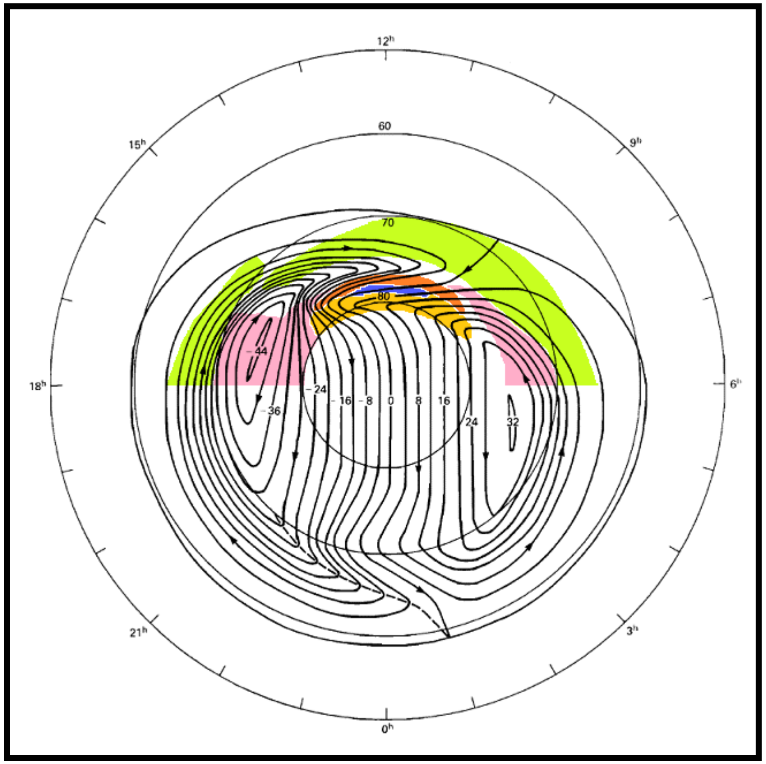

Dayside FAC System
***Erlandson et al.*, JGR, 1988**

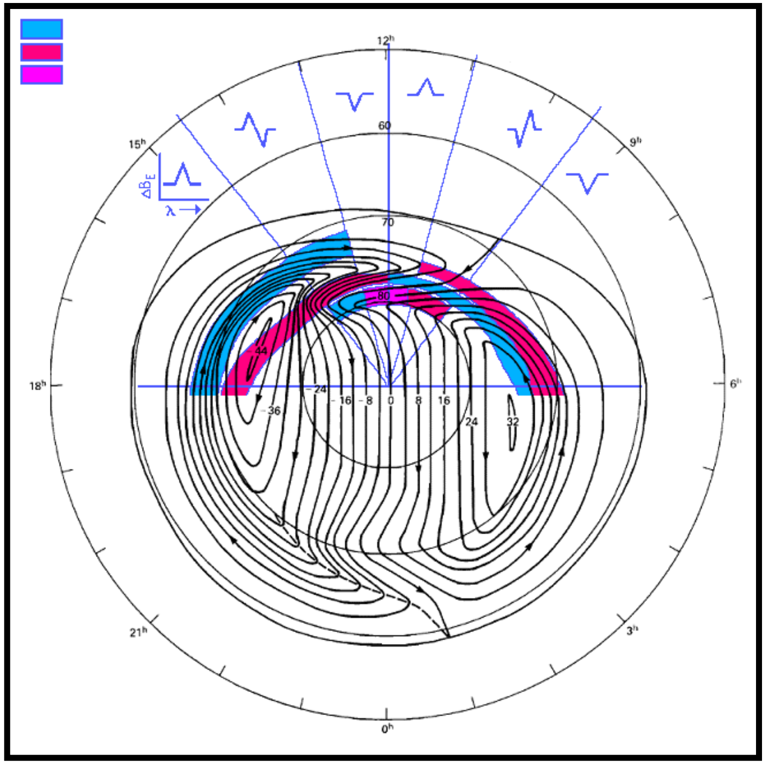

Heppner - Maynard Convection Patterns (JGR, 1987)

Aurorae and Polar Cap

Nopper and Carovillano, GRL 699, 1978

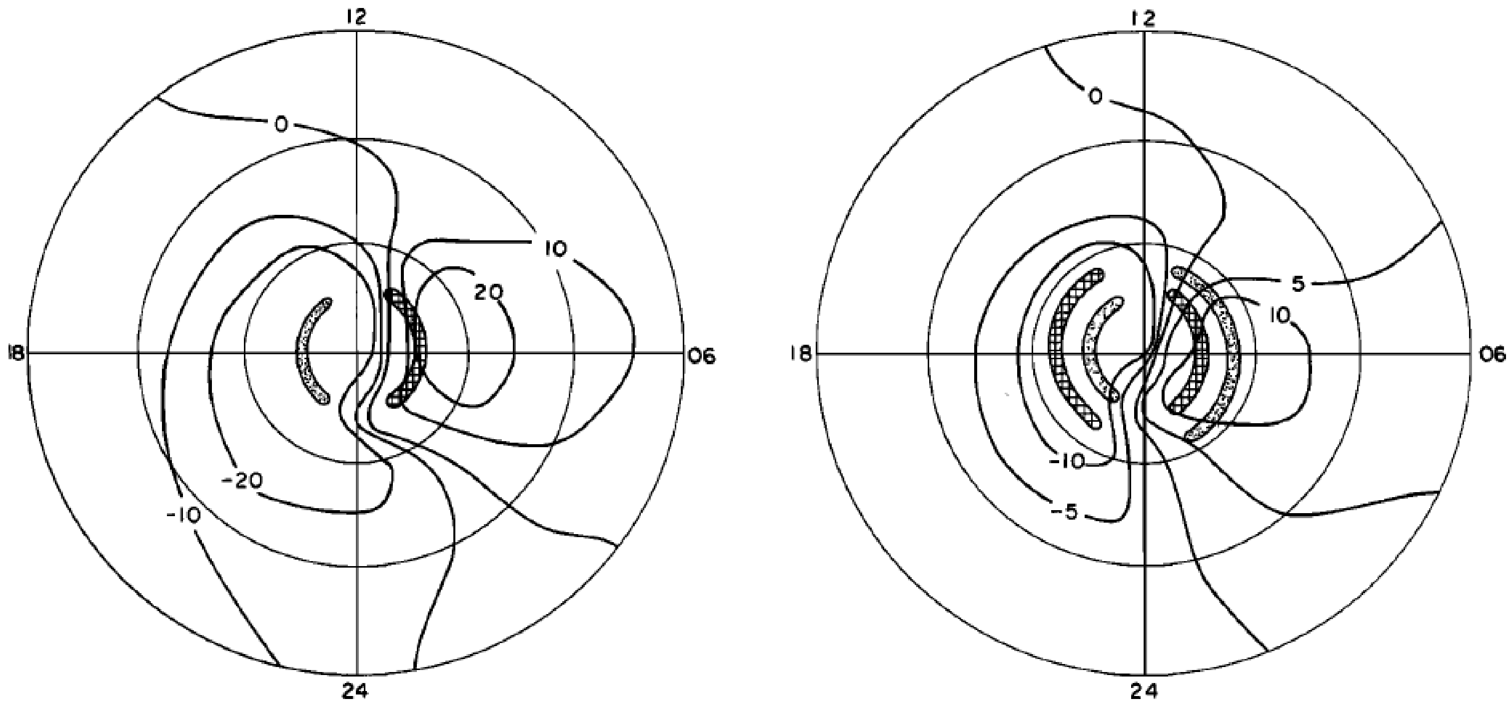

Region 1 = 10^6 A
Region 2 = 0 A

Region 1 = 10^6 A
Region 2 = $3 \cdot 10^5$ A

Wolf, R. A., Effects of Ionospheric Conductivity on Convective Flow of Plasma in the Magnetosphere, JGR, 75, 4677, 1970.

Aurorae and Polar Cap

Burke, Weimer and Maynard, JGR, 104, 9989, 1999.

Independent studies using AE-C, S3.2 and DE-2 measurements of Φ_{PC} all showed that the highest correlation was obtained with

LLBL potential **IEF**

$$\Phi_{PC}(kV) = \Phi_0(kV) + \alpha V_{SW} B_T Sin^2(\theta/2)$$

$$B_T = \sqrt{B_Y^2 + B_Z^2}$$

$$\theta = B_Z / B_T$$

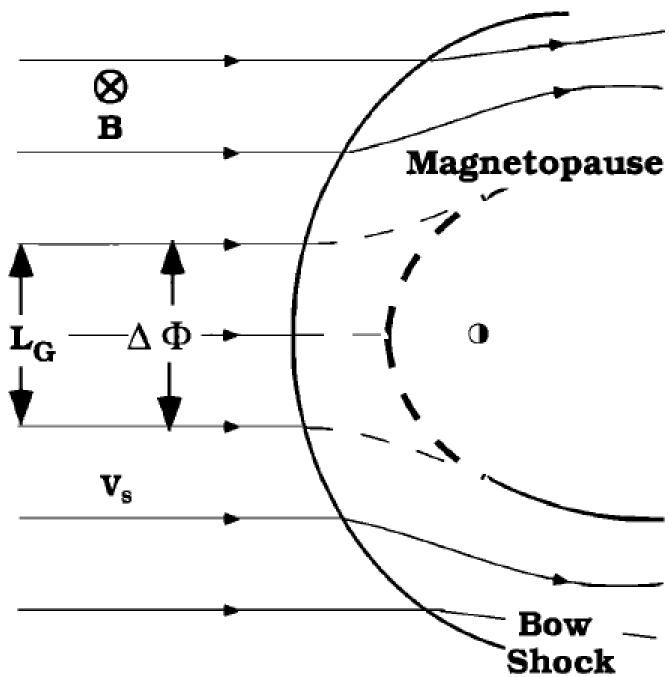

- **Interplanetary electric field (IEF) in mV/m. Since 1 mV/m $\approx$ 6.4 kV/ R_E**
- **L_G => width of the gate in solar wind (~ 3.5 R_E) through which geoeffective streamlines flow.**

Aurorae and Polar Cap

IMF $B_Y > 0$; $B_Z < 0$

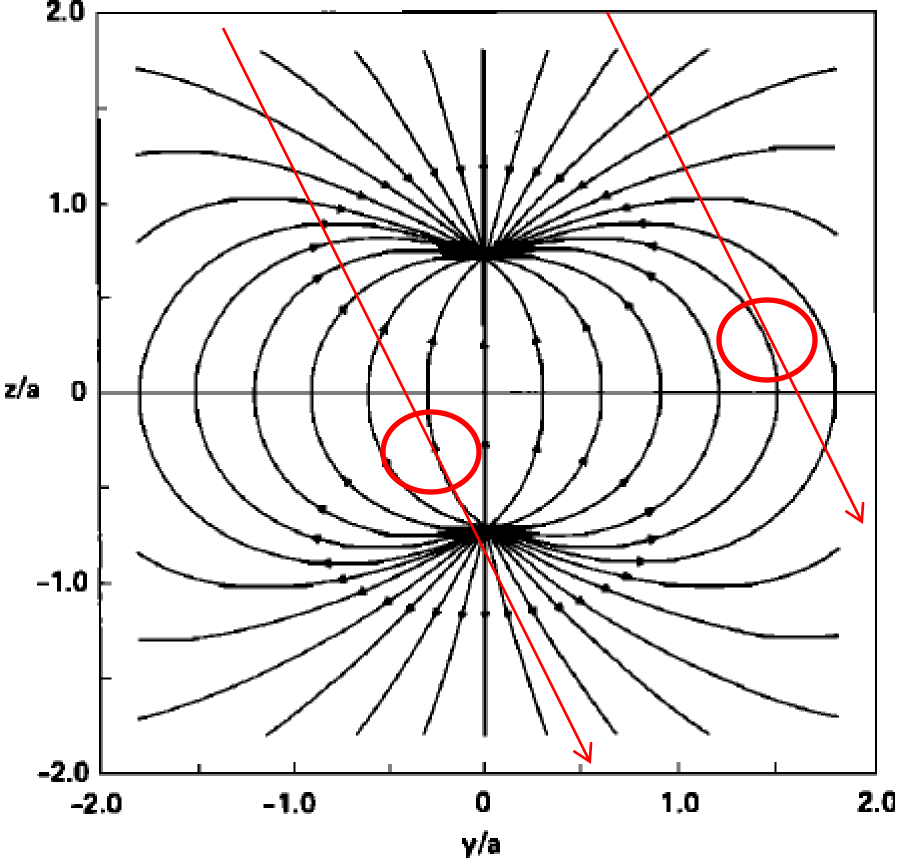

IMF $B_Y < 0$; $B_Z > 0$

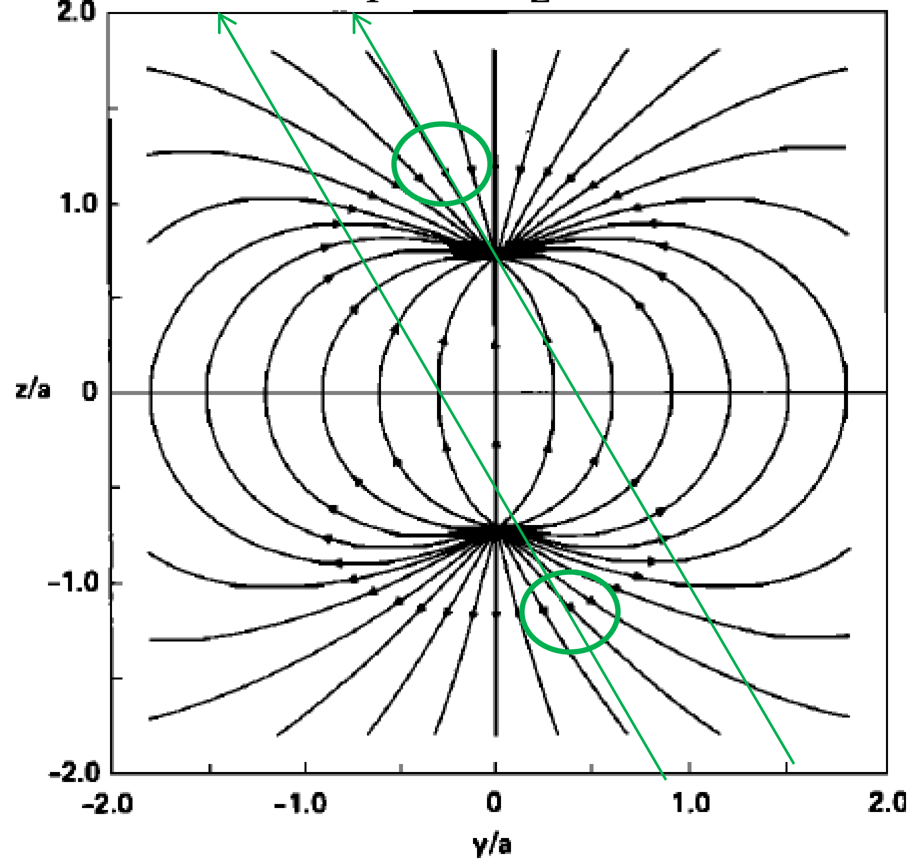

A second issue concerned the generalization of the *Dungey* model to 3D

- **Component merging hypothesis (*Bengt Sonnerup*)**
- **Anti-parallel merging hypothesis (*Nancy Crooker*)**

Aurorae and Polar Cap

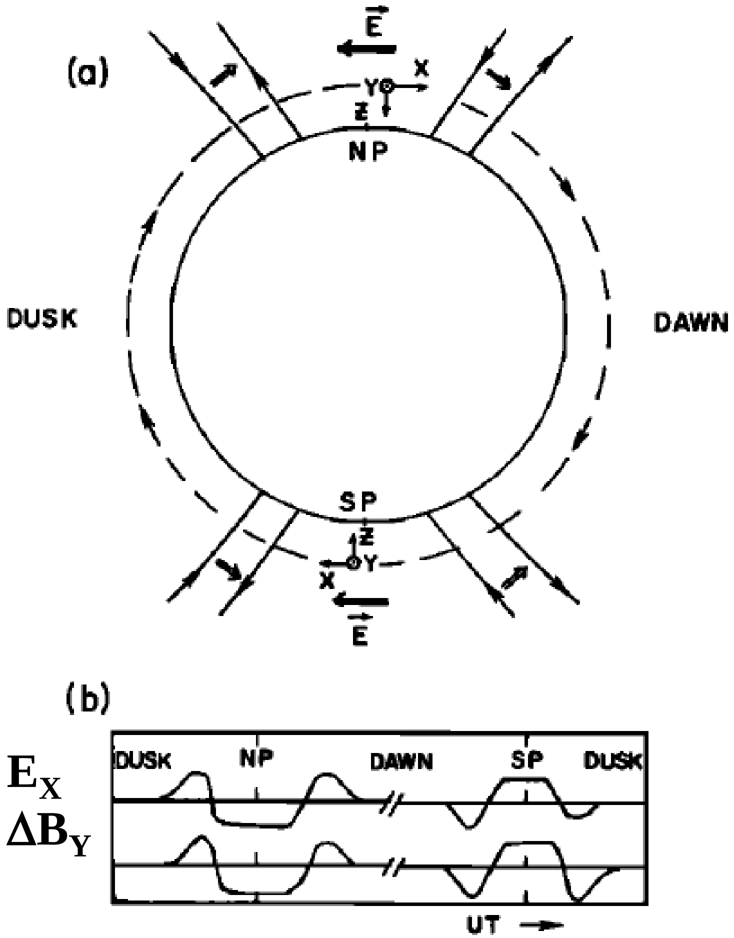

E_X

ΔB_Y

Aurorae and Polar Cap